UCRL- 92332
PREPRINT

GRAVITATIONAL COLLAPSE AND THE COSMIC ANTINEUTRINO BACKGROUND

S.E. Woosley
James R. Wilson
Ron Mayle

THIS PAPER WAS PREPARED FOR SUBMITTAL TO

ASTROPHYSICAL JOURNAL PART I

March 11, 1985

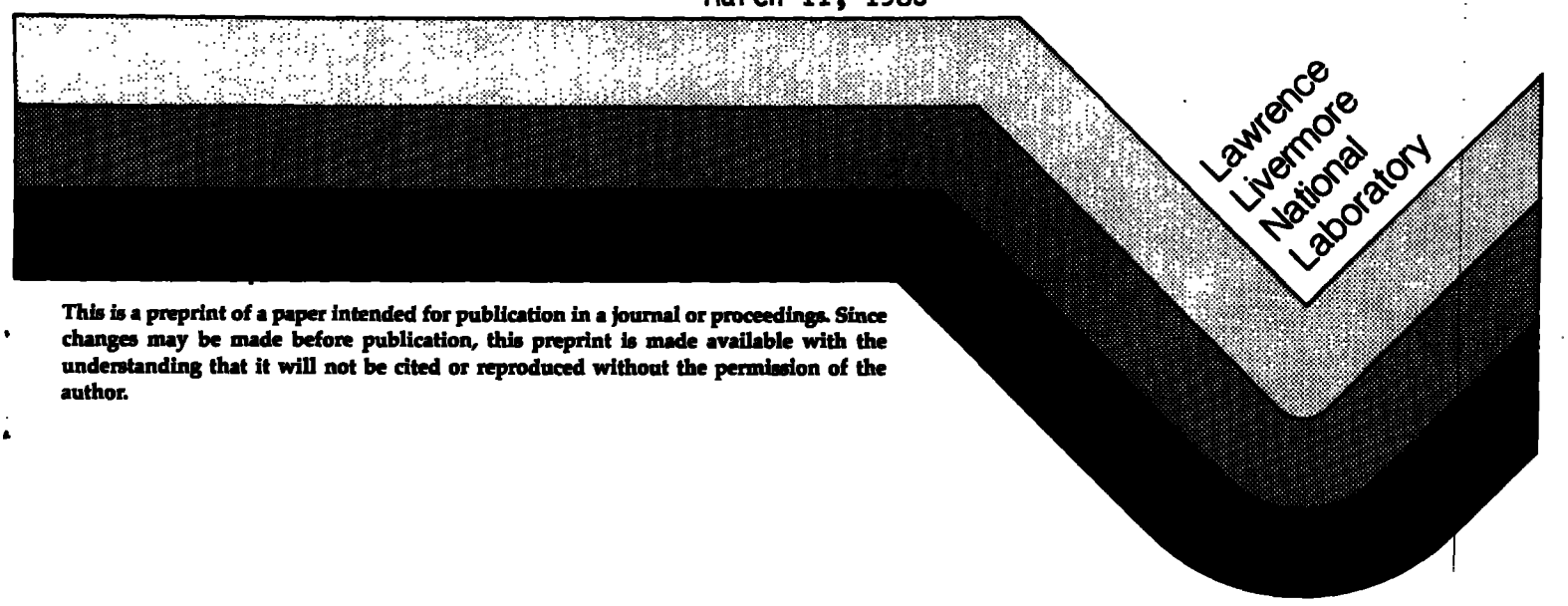

Gravitational Collapse and the Cosmic Antineutrino Background

S. E. Woosley

Board of Studies in Astronomy and Astrophysics, Lick Observatory
University of California, Santa Cruz CA 95064
and
Special Studies Group, Lawrence Livermore National Laboratory
Livermore, CA 95064

James R. Wilson

B- Division, Lawrence Livermore National Laboratory
Livermore, CA 94550

and

Ron Mayle

Physics Department
University of California, Berkeley CA 94720
and
B-Division, Lawrence Livermore National Laboratory
Livermore, CA 94550

ABSTRACT

During their collapse to neutron stars or black holes, stellar cores emit an intense flux of electron antineutrinos produced primarily by positron capture and pair annihilation. Providing that the typical energy of these neutrinos exceeds about 10 MeV, it has been suggested that the composite signal of all gravitational collapses that have ever occurred might be visible to detectors currently contemplated for the study of proton decay. Estimates of the antineutrino flux and spectra from Type II supernovae and the gravitational collapse of still more massive stars to black holes are obtained from numerical and semi-analytic calculations of models in the mass range 10 to 5×10^5 $M_\odot$. *The determined fluxes and spectra probably lie outside the range of detectability, at least in the near future.*

I. INTRODUCTION

As is well known, or at least *widely believed*, the sun continuously irradiates the Earth with a copious flux of electron neutrinos released as a byproduct of the nuclear fusion reactions transpiring in its core. The flux of these neutinos is such that no signal from any other credible astronomical source, except perhaps *Galactic* supernovae (Burrows 1984; Hillebrandt and Muller 1984), would compete in the same energy band, *i.e.* for energies less than about 10 MeV. Below about 3 MeV the Earth itself is also a prolific source of neutrinos and *anti*neutrinos produced by the decay of radioactive minerals (Krauss, Glashow, and Schramm 1984). Between 3 MeV and the much higher energies associated with neutrinos produced by cosmic ray air-showers in the Earth's atmosphere, there lies a window in which one may view the universe and its collective antineutino emissions. In this paper we present estimates of the flux produced by the gravitational collapse of massive stars throughout the course of cosmic evolution. This flux is characterized by energies $\lesssim$ 15 MeV, although the energy may be substantially less if the emitting objects lived their lives at a very early redshift, and originates not from any single event, but from the ensemble of all gravitational collapses that have ever occurred. Earlier papers (Bisnovatyi-Kogan and Seidov 1984 and references therein; Krauss, Glashow, and Schramm 1984) have pointed out that supernovae might produce a detectable signal in the antineutrino background and at least one experimenter (Dar 1984) thinks that he may have actually observed that signal. Here we calculate the electron antineutrino spectrum for a variety of collapses including implosions that do *not* produce visible supernovae (but may contribute to "dark matter"), and give numerical estimates of the estimated cosmic flux based upon several sets of asumptions.

II. ESTIMATES OF THE COSMIC ANTINEUTRINO BACKGROUND

All stars that have mass heavier than about 8 $M_\odot$ on the main sequence are expected to end their lives by collapsing to a compact object which may, depending on the particular stellar mass involved, be either a black hole or a neutron star. If one neglects, for the time being, the complicating effects of rotation, stars of 300 $M_\odot$ and greater are believed to collapse to black holes (Woosley and Weaver 1982; Bond, Arnett, and Carr 1982; Fuller, Woosley, and Weaver 1983, 1985), stars from 100 to 300 $M_\odot$ explode upon encountering the pair instability following helium core burning leaving no remnant (Barkat, Rakavy, and Sack 1967; Woosley and Weaver 1982; Bond, Arnett, and Carr 1982, 1984), and stars from 8 to 100 $M_\odot$ may, depending upon details of the late evolution (and the physics various researchers employ to study that evolution) become either neutron stars or black holes (*cf.* Bowers and Wilson 1982a; Wilson 1984; Hillebrandt 1984; Nomoto 1984). In all cases the final evolution of the star occurs very rapidly and the central regions are raised to high temperature by the gravitational contraction. Neutrinos are produced both by the annihilation of thermal pairs and, especially at high density, by the capture of pairs upon free nucleons. Depending upon specific assumptions one may reasonably make, quite variant values of integrated cosmic flux are obtained. For the most part, the strongest signals originate from processes that may have transpired early in the evolution of the universe as galaxies and stars were first forming.

a) The Conservative Approach

In the consideration of any costly experiment it is important to have a guideline, upon which most of the community would agree, as to the *minimum* expected signal. In short, what is the antineutrino flux currently being produced by events *that have been observed* (*e.g.* in the optical wavelengths) in the *present* universe? We claim that the only events satisfying this criterium are Type II supernovae. Type I supernovae, with their bright light curves powered by the radioactive decay of explosively synthesized ^{56}Ni and ^{56}Co (*cf.* Colgate and Mckee 1969; Axelrod 1980), are believed to be a consequence of the thermonuclear disruption of an accreting white dwarf star (*cf.* Whelan and Iben 1973; Woosley, Axelrod, and Weaver 1984; Nomoto, Thielemann, and Yokoi 1984). No neutron star or black hole remnant is left behind. The peak temperatures obtained during the explosion are limited by the thermal pressure required to initiate a dynamic expansion and by photodisintegration to $T \lesssim 0.7$ MeV. Thus the *thermal* antineutrino flux from Type I supernovae would be invisible against the large terrestrial background from β-decay (Krauss, Glashow, and Schramm, 1984). The neutrinos from electron capture in Type Is are limited by the relatively low Fermi energy at the time of the explosion (~5 MeV), the small Q-values for the capture, and

occurred in the observable universe. Owing to the expansion of the universe, only relatively nearby, recent supernovae will have spectra like Figure 1. More distant emissions will be red-shifted and thus the total spectrum from all distances will be both broadened and degraded in energy. This effect has been considered in detail by Bisnovatyi-Kogan and Seidov (1984) for various cosmological models with the conclusion that the mean neutrino energy is degraded by a factor ranging from 1/2 ($\Omega = 0$) to 3/5 ($\Omega = 1$; see also Krauss, Glashow, and Schramm 1984). One thus obtains a signal of cosmic antineutrinos peaked at $\sim$ 6 to 10 MeV with a flux

$$\phi_0 \sim 1.0\ cm^{-2}s^{-1}. \tag{1}$$

This admittedly conservative estimate is approximately two orders of magnitude smaller than obtained by Krauss *et al* (three orders smaller than in their original preprint which, in part, instigated our research on this subject) and Dar (1985) even though they employed arguments similar to ours. It also corresponds to a "mass" in electron antineutrinos presently of only $\sim 5 \times 10^{-37}$ g cm^{-3} or several thousand times less than estimated by Bisnovatyi-Kogan and Seidov (1984). The chief difference lies in the assumed *current* rate of Type II supernovae which we base upon luminosity density estimates rather than mass density and supernova rates per galaxy.

b) The Signal Expected From Galaxy Formation

The comparatively small size of our conservative estimate is a consequence of the present low rate of massive star formation in the universe. Less than about 5% of the mass of our own Milky Way presently resides in the interstellar medium (Gordon and Burton 1976), the remainder being locked up in low mass stars and perhaps some "dark matter" of unknown properties. This was not the case when the universe was young and galaxies were forming. One may estimate, with considerably greater uncertainty, the *total* number of stellar collapses that have ever occurred by assuming that all stars forming above a certain critical mass will collapse; that the "initial mass function" (IMF) has been constant with time; and that the IMF is the same throughout the universe. The latter two assumptions are difficult to justify (although see Scalo 1984), especially when one speaks of the very early universe. Silk (1977) and many others have presented arguments to suggest that more massive stars may have predominated in a hypothetical "Population III." Palla, Salpeter, and Stahler (1983), on the other hand, show that the cooling from molecular hydrogen may reduce the Jean's mass to a level where low mass stars *might* have formed. Essentially the IMF during galaxy formation is unknown. As a working hypothesis we assume that the IMF has been constant and is accurately represented by the work of Miller and Scalo (1979). We further assume that all stars heavier than 8 $M_\odot$ on the main sequence

most of all, by the low efficiency of converting rest mass to neutrinos ($\lesssim 10^{50}$ erg in a Type I explosion of the "deflagrating" variety as compared to $\sim 10^{53}$ erg of electron neutrinos and antineutrinos produced in a Type II explosion).

Supernovae Type II, on the other hand, do not occur in elliptical galaxies. They are found only in spiral and irregular galaxies and occur at a rate roughly proportional to the total *luminosity* of the galaxy (this is a better measure of the massive stellar population responsible for Type IIs than, for example, the galactic *mass*). The rate of Type II supernovae in spirals (especially $Sb - Sd$) is ~ 0.5 supernovae $(10^{10}$ $L_\odot)^{-1}$ (100 years)$^{-1}$ (Tammann 1982). The luminosity density of the universe *from the light emitted only by spiral galaxies* (excluding $S0$) is 5.6×10^7 $L_\odot$ Mpc^{-3} (Yahil, Sandage, and Tammann 1980). Those two numbers imply a supernova rate in the present universe of 3.0×10^{-86} cm^{-3} s^{-1}, a value that is probably accurate to a factor of three.

Next, we estimate the antineutrino signal expected from typical Type II supernovae. Recently Wilson (1984) and Wilson *et al.* (1985) have calculated the explosion of massive stars of 10, 15, and 25 $M_\odot$ and found that the properties of the (time integrated) antineutrino signal do not vary greatly from star to star (Table 1 and Fig. 1). Typically, the formation and cooling of the neutron star yields $\sim 3 \times 10^{53}$ erg, of which about 1/5 is emitted as electron antineutrinos having energy ~ 13 MeV. Actually, the explosions studied by Wilson were only calculated for about one second following core bounce during which only $\sim 10^{53}$ erg escaped. Thus $\sim 2/3$ of the values given in Table 1 for 10, 15, and 25 $M_\odot$ stars come from the extrapolation of the antineutrino fractional energy to the time when the neutron star has cooled completely. This is accomplished by holding the spectrum calculated at the last point constant until all the anticipated energy has been emitted. A similar spectrum has also been calculated by Nadezhin and Otroshenko (1980). We note that this corresponds to roughly 2% of the rest mass of the residual neutron star emitted as electron antineutrinos. If the core bounce mechanism does not succeed in producing mass ejection or if the remnant mass exceeds the critical value for a stable neutron star a black hole will form (Woosley and Weaver 1982). Accretion into the black hole may itself produce additional antineutrinos, a possibility discussed by Burrows (1985) and to which we shall return in a subsequent section. It should also be noted in Table 1 that the average neutrino energy for the 10, 15, and 25 $M_\odot$ stars is approximately 3 times the material temperature at the neutrinosphere. This is typical of a well defined neutrinosphere of near constant thermodynamic properties that exists in these "lower" mass stars. Later in §2*c* when we consider the emission accompanying the formation of massive black holes we shall find that a large fraction of the energy is released after the neutrinosphere temperature has started to decline. Hence the average neutrino energies for 150 and 500 $M_\odot$ models in Table 1 are considerably less than 3 kT.

To obtain the signal at Earth, one must sum over all collapses that have

will end their lives by collapsing and producing a signal like Figure 1 (actually, as we shall discuss in the next section, with the exception of stars in the 100 to 300 $M_\odot$ range, the signal would be somewhat stronger if that collapse did *not* produce an outgoing shock wave and supernova explosion). According to Miller and Scalo, ~10% of the mass that goes into stars is formed into stars heavier than 8 $M_\odot$. This value includes the effect of recycling. The slope of the integrated Miller-Scalo IMF near 10 $M_\odot$ is approximately -1.7 and falls off rapidly at higher masses. Integrating their IMF implys a typical stellar mass (by number) above 8 $M_\odot$ of ~15 $M_\odot$. The time integrated number density of gravitational collapses in the universe is then

$$N = 2.9 \times 10^{-65} \Omega_b h_{55}^2 \; cm^{-3} \tag{2}$$

where h_{55} is the Hubble constant in units of 55 km s^{-1} Mpc^{-1} and Ω_b is the ratio of the baryon density of the universe to the Einstein deSitter value. For $\Omega_b = 0.1$ and $h_{55} = 1$, this number density is 250 times greater than the present Type II supernova rate given in the previous section integrated over the ~12 by (if $1 = \Omega >> \Omega_b$ is adopted) lifetime of the universe and would imply an antineutrino signal

$$\phi_{GF} \sim 250 \; cm^{-2} s^{-1}. \tag{3}$$

A similar, although slightly smaller value can be obtained from nucleosynthetic arguments. We assume, as is the common paradigm, that the heavy elements from oxygen through calcium are a product of stellar evolution and Type II supernovae in the 8 to 100 solar mass range. We recognize, of course, that this is not a unique solution. Stars in the 100 to 300 $M_\odot$ range, if they ever existed in sufficient numbers, could make the same species (Woosley and Weaver 1982), but it seems reasonable that the most common stars seen today have played a substantial role in producing the heavy elements. One needs to produce a metallicity, Z (chiefly the abundance of ^{16}O), in the universe of about 1% or, again adopting $h_{55} = 1$, $\Omega_b = 0.1$, a mass density 5.7×10^{-33} g cm^{-3} of heavy elements. Weaver and Woosley (1980) have determined that the fraction of mass ejected by massive star in the form of heavy elements is given approximately by $z_{ej} = 0.5 - 6 \; M_\odot/M$ where M is the main sequence mass of the star. Thus a 15 $M_\odot$ supernova ejects about 1.5 $M_\odot$ of heavy elements, a 25 $M_\odot$ star ejects 6.5 $M_\odot$, *etc.* Combining this expression with the Miller and Scalo IMF gives a typical nucleosynthetic supernova mass of ~25 $M_\odot$ and a typical mass ejected in the form of heavy elements of 6.5 $M_\odot$. The observed abundance of heavy elements then implies an integrated number density of gravitational collapses of 4.4×10^{-67} cm^{-3}, or about one sixth of equation (2), and thus a nucleosynthetic flux

$$\phi_N \sim 40 \; cm^{-2} s^{-1}. \tag{4}$$

A similar value ($\phi \sim 70\ cm^{-2}\ s^{-1}$) can be obtained using equation (5.2) of Carr, Bond, and Arnett (1984) with $Z_{max} = 0.01$ and values for Q_{tot} and $\langle \epsilon_\nu \rangle$ from Table 1. Actually there will be many more lighter supernovae that do not produce as much heavy elements as a 25 $M_\odot$ star, thus equation (4), which is weighted by the mass of heavy elements ejected, is an underestimate and a value closer to equation (3) is to be preferred.

The fluxes given in equations (3) and (4) both correspond to emission at a very specific epoch, however, and the red-shift factor used for equation (1) is not appropriate (Bisnovatyi-Kogan and Seidov 1984). In particular the antineutrino energies must be degraded by a red shift appropriate to the era when most of the baryonic matter in the universe first went into stars which presumably is approximately concordant with the age of galaxy formation. This is a highly uncertain number. In fragmentation models (*e.g.* the "pancake" model as updated for massive neutrinos by Doroshkevich *et al.* 1981), galaxy formation is triggered by the collapse of larger structures. The low density of such structures tells us that they must have formed at close to the present time with an upper limit on formation red shift $z_f \sim 3$. Other views of galaxy formation, *e.g.* heirarchical clustering (White and Rees 1978), place the formation epoch of galaxies at earlier times, say $z_f \gtrsim 5$. Measurements by Djorgovski and Spinrad (1985) of the magnitudes and colors in the visible regime for distant radio galaxies are consistant with a model in which galaxies formed at $z_f \sim 5$. Obviously a major goal of antineutrino astronomy, if feasible, would be the attempted definition of the epoch of galaxy formation by studying precisely that flux which we now derive. An unambiguous detection would give unique and valuable insight into the early evolution of the universe. On the other hand, that same red shift may degrade the signal to such low energies ($\lesssim 3$ MeV) that it becomes invisible against the terrestrial background from β-decay (Krauss, Glashow, and Schramm 1984). In particular if the redshift is 3 or less the signal from collapses shown in Figure 1 might be visible, but if star formation occurred much earlier an increasingly large fraction of the flux given in equation (3) would fall in an unobservable waveband.

c) Antineutrinos From Black Hole Formation; Limits on the "Missing Mass"

When a black hole, or more appropriately "trapped surface," forms in the interior of a collapsing massive (or super-massive) star, the plasma that accretes into that black hole is generally very hot, if only owing to the effects of geometrical compression, and quite optically thick to photons. Thus, in principal, a substantial fraction of the rest mass energy could be emitted as neutrino pairs. Working against this possibility is the trapping of neutrinos at high density by the streaming matter so that they do not escape but are advected into the hole, and the incomplete thermalization

of the streaming velocity. Furthermore, unless the temperature becomes very high, the time scale for losing a substantial fraction of the thermal energy of the plasma by neutrino emission may be long compared to that for gravitational collapse so that, again, the energy potentially available is simply lost to the hole (see also Burrows 1985). Without a detailed model it is difficult to estimate the relative efficiencies of these various factors, but in principal, a very large antineutrino background is possible. The anticipated flux may be expressed

$$\begin{aligned}\phi_{col} &= \frac{\rho_c \Omega_{col} c^3 Q_{rem}}{\epsilon} \\ &= 9.6 \times 10^3 \left(\frac{Q_{rem}}{0.01}\right)\left(\frac{\Omega_{col}}{0.1}\right)\left(\frac{10\,MeV}{\epsilon_{10}}\right) h_{55}^2\ cm^{-2} s^{-1},\end{aligned} \tag{5}$$

where ρ_c is the critical closure density for an Einstein deSitter cosmology, Ω_{col} is that fraction of the closure density provided by collapsed objects, Q_{rem} is that fraction of the rest energy of the remnant mass that is converted into antineutrinos during the course of collapse, and ϵ_{10} is the mean energy of those antineutrinos in units of 10 MeV. Additionally, since a large fraction of the collapses presumably transpired early in the universe, one must divide the mean antineutrino energy by a factor $(1+z_f)$ where z_f corresponds to the specific epoch when the collapsed objects formed. A choice of unity for the various factors in parentheses would obviously lead to a much greater signal than discussed in the previous section.

The collapse to a black hole may occur in either of two situations. For stars in the mass range 8 to 100 $M_\odot$ the iron core first collapses, forming a hot extended neutronized sphere which has, at its center, near nuclear density. If the reflected shock and neutrino transport are inadequate to eject the overlying mantle and envelope of the star, an accretion shock develops and a supernova of the ordinary variety is avoided (although see Bodenheimer and Woosley 1983). Initially the matter falls through the accretion shock onto the hot neutron sphere and its mass grows. Eventually sufficient matter accretes and sufficient cooling and deleptonization occurs that the object collapses inside the Schwartzschild radius and becomes a black hole. Following that, the remainder of the star accretes into the black hole at a variable rate depending most critically upon its initial density profile. No realistic calculation of the evolution even up to the development of a trapped surface has been carried out, although Woosley and Weaver (1982) have studied the accretion stage in a "failed" 25 $M_\odot$ supernova model for several seconds following the core bounce. Material passing through the shock is heated to temperatures $\sim$ 2 MeV in a region that is thin to this emission. Further compression behind the shock may lead to still greater temperatures as the hot neutron star loses energy and becomes a black hole.

The time required to become a black hole is governed by the rate at which the neutronized core can radiate away its gravitational binding energy as neutrinos

(essentially a Kelvin-Helmholtz time), but even relatively stiff nuclear equations of state cannot support a neutron star once its gravitational binding energy has reached $\gtrsim 20\%\ Mc^2$. Since the formation of a trapped surface, when it occurs, is likely to lead to the collapse of the core on approximately a hydrodynamic time scale, $\lesssim 10^{-4}$ s, far less than a neutrino diffusion time, this 20% represents a rough upper bound to the total energy that can be radiated in all forms of neutrinos. Assuming three flavors of neutrino pairs suggests an upper limit close to 3% of the rest mass for emission as electron antineutrinos. The mass involved is at most a few solar masses, so in fact the energy obtained from a "failed bounce" is only sightly larger than for the ordinary supernovae discussed before (see Fig. 1 and Table 1).

Additional neutrino emission might be expected from the remainder of the presupernova star, its mantle and envelope, as they accrete into the black hole. The mass available for producing neutrinos in this fashion is limited, however, to material at relatively high density and the net efficiency turns out to be small. We will return to this issue of black hole accretion in a more quantitative fashion shortly, especially for large stars. We note in passing, however, that *both* black hole formation *and* mass ejection powered by a reflected shock are, contrary to popular opinion, *not* necessarily mutually exclusive occurrences. If an outgoing shock leaves behind a remnant mass greater than allowed for a stable neutron star but travels sufficiently far that the mantle of the star has already achieved escape velocity before that core can deleptonize and collapse, then a visible supernova and explosive nucleosynthesis can result even though the remnant is a black hole. Calculations to further explore this proposition are in progress (Wilson *et al.* 1985). The time scales for cooling and deleptonization (*i.e.*, for a neutrino to diffuse out of the core) and for the shock to traverse the mantle are comparable, both on the order of a second.

A second scenario for black hole formation utilizes stars having main sequence mass greater than 300 $M_\odot$(Woosley and Weaver 1982; Bond, Arnett, and Carr 1982, 1984). For stars between 100 and 300 $M_\odot$ the evolutionary endpoint is a pair instability supernova (*cf.* Barkat *et al* 1967). The temperatures generated in the explosion, $T \lesssim 0.4$ MeV, are limited by that value which would promote endoergic silicon burning and photodisintegration, thus leading to collapse. The neutrinos from such events therefore have too little energy to be observed. Non-rotating stars with greater mass, however, will collapse directly to a black hole, either owing to the electron-positron pair instability encountered at the end of helium core burning ($300 \lesssim M/M_\odot \lesssim 10^4$) or the post-Newtonian gravitational instability during helium burning ($10^4 \lesssim M/M_\odot \lesssim 10^5$; Fuller, Woosley, and Weaver 1983, 1985) or prior to hydrogen ignition ($M/M_\odot \gtrsim 10^5\ M_\odot$; Iben 1963; Fowler 1966). Once initiated, the collapse of non-rotating stars of such enormous mass proceeds smoothly to trapped surface formation. In particular, no strong accretion shock is formed and heating is principally due to geometrical compression. The collapse is quite non-homologous, however, (Fuller, Woosley, and

Weaver 1985) with ≲20% of the inner star collapsing as a unit by the time the event horizon forms (see also §IIe).

The formation of a "neutrino fireball" during the collapse of "very massive objects" ($300 \lesssim M/M_\odot \lesssim 10^4$) has been examined by Bond, Arnett, and Carr (1984) and Woosley and Weaver (1982 and unpublished). As specific numerical examples we consider here the evolution through collapse and black hole formation of two helium cores having initial total masses 150 $M_\odot$ and 500 $M_\odot$ (Fig. 2). The physics employed in these computational studies has been described by Woosley and Weaver (1982) and Bowers and Wilson (1982b). Following their stable evolution through hydrostatic helium burning, the cores encounter the pair instability and begin to collapse rapidly. Nuclear burning at around 250 to 400 keV slows this collapse somewhat (in lighter helium stars that encounter this instability nuclear burning produces an explosion) as does the diminishing strength of the instability (see Barkat *et al.* 1967). Once the pairs that are created are very relativistic, the energy lost to creating their rest mass is of decreasing importance. Following the initial collapse, which is nearly homologous in the 150 $M_\odot$ model, a state of near hydrostatic equilibrium is re-established in the central regions when the central temperature has reached about 600 keV and the density, $10^7\ g\ cm^{-2}$ (see Fig. 2). This state persists until the central temperature has rises to about 1 MeV. A similar evolution characterizes the 500 $M_\odot$ model.

Continued and accelerating collapse is then caused by the *photodisintegration*, first of nickel into α-particles and, later, alphas to nucleons and, to a lesser extent, by neutrino losses. Typical speeds of infall during this epoch range between about 1 and 3×10^9 cm s^{-1} and the central temperature rises to ~3 MeV as a neutrino photosphere or "neutrinosphere" first forms. The collapse is not at all homologous throughout the star during this stage. Only about the inner 20% is collapsing homologously in the 150 $M_\odot$ model as the central temperature rises to 5 MeV and this fraction decreases still further as the evolution proceeds. A trapped surface first forms at about 7 $M_\odot$ in the 150 $M_\odot$ model and about 10 $M_\odot$ in the 500 $M_\odot$ model (Fig. 3). At this point the central density has reached approximately the nuclear value, but the neutrinosphere still lies well outside the event horizon at ~10 $M_\odot$ and 250 km in the 150 $M_\odot$ model and ~ 24 $M_\odot$ and 520 km in the 500 $M_\odot$ model. The electron antineutrino luminosity at maximum is ~ 10^{54} (~ 5×10^{54}) erg s^{-1} and the *total* neutrino luminosity is ~ 6×10^{54} (15×10^{54}) erg s^{-1} in the 150 $M_\odot$ (500 $M_\odot$) model. In the 150 $M_\odot$ model at peak neutrino luminosity, roughly 2/3 of the emission is in the form of μ and τ-neutrinos and 1/6 each in the form of electron neutrinos and antineutrinos. In the 500 $M_\odot$ model at peak, 1/3 of the energy is in the form of μ and τ-neutrinos and 1/3 each in electron neutrinos and antineutrinos. The difference arises because of the differing entropies in the two models. The temperature at the neutrinosphere is ~ 4 MeV in both cases. Figure 1 gave the total time integrated energy spectrum of these two collapses. Figure 4 gives the integrated spectrum at 3 times for the 150 $M_\odot$

model. This sort of luminosity and spectrum persist as the next 10 $M_\odot$ or so of the star accretes into the black hole which transpires in a time $\tau_{acc} \sim R(m)/v(m) \sim 0.1$ s.

As the accretion rate slows, owing to the decreasing density and extended radius of the accreting matter, and the black hole mass grows, the neutrinosphere eventually moves inside the event horizon and the luminosity drops. Our calculations indicate that this occurs when roughly 20 $M_\odot$ (30 $M_\odot$) has accreted into the hole in the 150 $M_\odot$ (500 $M_\odot$) model. Thus for these two models $Q_{rem} \sim 0.0003$ and 0.0012 (assuming that the entire star accretes) and $\epsilon_{10} \sim 0.5$ are appropriate for equation (5) as Table 1 shows.

To verify the accuracy of the Wilson-Bower's supernova code for times near and following the collapse of the neutrinosphere inside the event horizon, the evolution of the deep interior of the star was recalculated using a different program that solved, in an instantaneous steady state approximation, the relativistic Bondi accretion problem (Michel 1972). Input parameters: the mass of the central object; density, temperature, and radius at the sonic point; and Γ, as defined by $P/\rho = (\Gamma - 1)\epsilon$, with P the pressure and ϵ the internal energy, were taken from the output of the Bowers and Wilson code. Admittedly the assumption of constant Γ is not an exact one but should suffice for present purposes. When a neutrinosphere is present, the antineutrino luminosity is calculated using

$$L_\nu = 4\pi \left(\frac{7}{16}\right) r_\nu^2 \, \sigma \, T_\nu^4 \left(1 - \frac{2GM_\nu}{r_\nu c^2}\right)\left(\frac{1 + v_\nu/c}{1 - v_\nu/c}\right), \tag{6}$$

where r_ν, T_ν, M_ν, and v_ν are the radius, temperature, interior mass, and velocity evaluated at the neutrinosphere defined by

$$\tau_\nu = \int_{r_\nu}^{\infty} \kappa_\nu \rho \, dr = 2/3. \tag{7}$$

The cross sections for neutrino interaction with nucleons and electrons are respectively (Tubbs and Schramm 1975; Bowers and Wilson 1982b)

$$\begin{aligned} \sigma_{p,n} &= 1.33\,\sigma_0 \left(\frac{E_\nu}{mc^2}\right)^2, \\ \sigma_e &= \left(\frac{3}{8}\right)\sigma_0 \frac{E_\nu kT}{(mc^2)^2} \end{aligned} \tag{8}$$

where $\sigma_o = 1.7 \times 10^{-44}$ cm^{-2} and $\mathrm{Sin}^2\theta_W = 0.25$ have been adopted. The cross section for absorption on nucleons, $\sigma_{p,n}$, given in the above equation is strictly for charged current interaction with nucleons. It should be multiplied by an additional factor of 1.39 to account for neutral current scattering interactions with both neutrons and protons. For positrons, the cross section is similar to that for σ_e but with a factor

of (7/8) replacing (3/8). Assuming that the neutrinos are in thermal equilibrium we have $< E_\nu >= F_4(0)/F_3(0)\ kT = 4.10\,kT$, where $< E_\nu >$ is the total energy in neutrinos divided by the total number of neutrinos and F is the Fermi Function, and $< E_\nu^2 >= F_5(0)/F_3(0)\ (kT)^2 = 20.81\ (kT)^2$. An energy weighted average has been employed because we wish ultimately to calculate a luminosity. Thus the total neutrino opacity is

$$\kappa_\nu = 7.9 \times 10^{-19} T^2_{MeV}(1 + 1.0 \times 10^7 \frac{T^3_{MeV}}{\rho})\ cm^2\, g^{-1}, \tag{9}$$

For optically thin systems the electron scattering term, $1.0 \times 10^7\ T^3_{MeV}$ should be replaced by the pair emission value, $7.6 \times 10^5\ T^3_{MeV}$.

When no neutrinosphere is present then the lower limit to the integral in equation (7) is replaced by the Schwartzschild radius and the luminosity calculated using Kirchhoff's Law

$$L_\nu = 4\pi(\frac{7}{16})ac \int r^2 \kappa_\nu \rho T^4 e^{-\tau}(1 - \frac{2GM(r)}{rc^2})^{\frac{1}{2}}(\frac{1 + v(r)/c}{1 - v(r)/c})dr. \tag{10}$$

with the lower bound on the integral taken at the event horizon. Good agreement is found between the values of L_ν in the Bowers and Wilson output and the accretion code calculated at times sufficiently late that the accretion flow has approached steady state. Figures 5, 6, and 7 show the evolution of some critical quantities in the 150 and 500 $M_\odot$ helium core studies.

d. Analytic Approximations

The general nature of these numerical results may be understood, especially for the very massive (pair unstable) stars, in terms of approximate analytic arguments. We first explore the relevant physical parameter space as displayed in Figures 8 and 9. Collapse of the cores proceeds isentropically, at least initially, since the time scales for neutrino losses (and certainly photon diffusion) are much longer than the free fall time scale (Fowler and Vogl 1964)

$$\tau_{ff} \sim (24\pi G\rho)^{-1/2} = 446\, \rho^{-1/2}\ s, \tag{11}$$

where τ_{ff} is a typical e-folding time for density increase and ρ is the local density. The total entropy is approximately constant throughout the mass of the initial model owing to the nearly uniform convective transport of energy prior to collapse. Typical values of total dimensionless entropy (S/Nk) range from 15 in the 150 $M_\odot$ helium core to 25 in the 500 $M_\odot$ helium core all the way up to 200 in a collapsing 10^5 $M_\odot$

supermassive star (Fuller, Woosley, and Weaver 1983, 1985). Entropies in the lower part of this range also characterize the (shocked) matter collapsing in a 10 to 100 $M_\odot$ star (Woosley and Weaver 1982). Paths of constant entropy are shown in Figure 9 for material consisting of a gas of free nucleons ($Y_e = 0.5$), radiation, and relativistic pairs, for which, according to Bond, Arnett, and Carr (1984):

$$\begin{aligned} S_{tot} &= S_{pair} + S_\gamma + S_{nucleon} \\ S_\gamma + S_{pair} &= (1 + 7/4)(1.906 \times 10^8\, T^3_{MeV}/\rho) \\ S_{nucleon} &= 8.7 + 0.5\, ln\,(S_{pair} + S_\gamma) - 0.5\, ln\,(\rho/10^{10}\ g\ cm^{-3}). \end{aligned} \tag{12}$$

As the temperature of this gas rises owing to adiabatic compression, the neutrino losses from pair annihilation and capture on nucleons become substantial. When the evolutionary path reaches an approximate balance of collapse time scale (eq. 11) and neutrino cooling time scale, the contraction ceases to be adiabatic and the core increases rapidly in density at almost constant temperature. Pair losses occur at a rate (Bowers and Wilson 1982b)

$$\epsilon_{pair} = 2.0 \times 10^{25}\, T^9_{MeV}\ erg\ cm^{-3} s^{-1}. \tag{13}$$

Even larger energy losses occur at high density because of the capture of pairs on neutrons and protons. In preparing Figure 9, the rates for these capture losses were calculated assuming a nucleon gas of equal numbers of neutrons and protons and rates from Fuller, Fowler, and Newman (1982ab; 1985). In the numerical models themselves neutrino transport and capture were calculated as described by Bowers and Wilson (1982b). Neutrino cooling times, given by the ratio of internal energy to neutrino energy loss rate, were estimated including the internal energy of the radiation (aT^4), nucleons ($3/2 N_A \rho k T$), the degeneracy energy of the electrons or pairs ($3/4 \eta k T \rho N_A Y_e$ with $Y_e = 0.5$) when they were degenerate, and their relativistic energy ($E_{rel} = (7/4) aT^4$) otherwise. As the isentropic tracks encounter regions where energy loss occurs so rapidly as to deplete the internal energy on a free fall time scale (Fig. 9), the general evolution towards higher temperatures is halted. Especially if the losses can deplete the energy in a fraction (say 1/5) of the free fall time pressure support is lost and the matter begins to collapse freely. Compression cannot regenerate the energy as fast as neutrinos remove it so the matter collapses to high density at nearly constant temperature.

As the density climbs the neutrinos soon become trapped due to scattering with nucleons and electrons. Even at relatively low densities the neutrino opacity may become quite large at high temperatures owing to the creation of pairs. Curves defined by the condition that neutrino diffusion time, $\tau_{DIF} \sim \kappa_\nu \rho L^2/c$, equal free fall time (eq. 11) or one-fifth free fall time are given in Figure 9 for representative length scales, 10^7 and 10^8 cm. Somewhere typically between the two lines shown in the

figure a neutrinosphere will develop. Thereafter the energy of the escaping neutrinos will no longer increase greatly, but will instead be set by conditions of near thermal equilibrium. We see that a common limit of ~3 to 5 MeV is expected for the free streaming case in very massive objects (see also Bond, Arnett, and Carr 1984). Higher temperatures imply such efficient neutrino production that cooling would occur on a small fraction of a collapse time scale. Densities above about 10^9 to 10^{10} g cm^{-3} imply substantial neutrino production by electron capture but also lead to an "optically thick" neutrinosphere as well. As we shall show, the emission temperature of the neutrinosphere is also limited to a value near 4 MeV. Thus general considerations suggest that the neutrinos observed from very massive stars will have originated at almost unique thermodynamic conditions.

Those conditions can be parametrized in terms of an accretion rate and other physical quantities. Consider a core that is accreting extremely optically thick matter at a rate $\dot{m} = 4\pi r^2 \rho(r) v(r)$. Introduce a parameter, $f = (v/v_{ff})^2$ where v_{ff} is the local free fall speed at radius r and v is the actual speed. In nature, of course, f will be a complicated function of position and time, but here we shall assume that it is constant in the region of interest. It will turn out that our principal results are not overly sensitive to f and its variations. We further assume that we are operating in a restricted portion of parameter space (Fig. 8) where the internal energy is predominantly in the form of radiation and relativistic pairs, hence conservation of energy and neglecting the small fraction of internal energy lost to neutrinos implies at radius r

$$E_{int} = \frac{GM(r)(1-f)}{r} \sim \frac{11}{4} a \left(\frac{T^4}{\rho}\right). \tag{14}$$

We further assume that in the vicinity of the neutrinosphere the density scales as some power law, *i.e.*, $\rho = \mathrm{Kr}^{-n}$ for a constant time slice. In fact, the power law dependence of ρ too is quite approximate and, even then, time and spatially varying. Early on n is not too different than for a polytrope, *i.e.*, $n \sim 3$. As the collapse advances, however, n is related to the pressure deficit and the equation of state of the gas (Brown, Baym and Bethe 1982). Yahil (1984) claims that $\rho \sim r^{-2/(2-\gamma)}$ with γ the adiabatic index. In general, n decreases, eventually approaching ~1.5, the free streaming limit, in the matter near the event horizon once a black hole forms. In what follows we adopt, unless otherwise specified, a median value $n = 2.2$, as is typical in the computer print out, at least at times and locations sufficiently well removed from the event horizon. Then the definition of neutrinosphere (eq. 7) and restriction of opacity to the first term of equation (9) implies a radius where neutrinos become trapped

$$\begin{aligned} r_\nu &= 8.0 \times 10^5 (1-f)^{2/7} f^{-3/7} \left(\frac{2}{3n-1}\right)^{4/7} M_\nu^{-1/7} \dot{m}^{6/7} \ \ cm \\ &\sim 4.3 \times 10^7 \left(\frac{\dot{m}}{100}\right)^{6/7} \left(\frac{M_\nu}{10}\right)^{-1/7} \ \ cm \end{aligned} \tag{15}$$

where M_ν, the interior mass, and $\dot{m}$, the accretion rate, are both in units of solar masses (per second for $\dot{m}$) and are to be evaluated at the neutrinosphere. The second line in the above and following equations reflect approximate evaluations assuming $f \sim 0.1$ and $n \sim 2.2$. The definitions of f and $\dot{m}$ along with the assumed equation of state (relativistic pairs and radiation only) further specify the temperature and density at the neutrinosphere

$$\begin{aligned} T_\nu &= 8.8\ (1-f)^{1/14} f^{1/7} (\frac{3n-2}{2})^{5/14} M_\nu^{3/14} \dot{m}^{-2/7}\ \ MeV \\ &\sim 4.0\ (\frac{\dot{m}}{100})^{-2/7} (\frac{M_\nu}{10})^{3/14}\ \ MeV, \\ \rho_\nu &= 1.4 \times 10^{10}\ (1-f)^{-3/7} f^{1/7} (\frac{3n-1}{2})^{6/7} M_\nu^{-2/7} \dot{m}^{-2/7}\ \ g\ cm^{-3} \\ &\sim 3.4 \times 10^9\ (\frac{\dot{m}}{100})^{-2/7} (\frac{M_\nu}{10})^{-2/7}\ \ g\ cm^{-3}. \end{aligned} \tag{16}$$

This radius and temperature can further be used to estimate a luminosity in the form of electron antineutrinos *if the emission is that of a blackbody.* From equation (6) and neglecting relativistic corrections,

$$\begin{aligned} L_\nu &= 4\pi (\frac{7}{16}) r_\nu^2 \sigma T_\nu^4 \\ &= 2.2 \times 10^{52}\ (1-f)^{6/7} f^{-2/7} (\frac{3n-1}{2})^{2/7} M_\nu^{4/7} \dot{m}^{4/7}\ \ erg\ s^{-1} \\ &\sim 2.6 \times 10^{54}\ (\frac{\dot{m}}{100})^{-4/7} (\frac{M_\nu}{10})^{-4/7}\ \ erg\ s^{-1}. \end{aligned} \tag{17}$$

It should be noted that equations (15) - (17) are to be used only when a neutrinosphere exists and neutrino losses do not greatly modify the internal energy near the neutrinosphere. For $\dot{m}$ too small to satisfy this criterium, dynamical arguments must be employed (Fig. 9). We note, where valid, that the dependence upon f and n is so weak that the expressions essentially relate neutrinosphere quantities to the accretion rate and interior core mass. In actual practice the accretion rate, too, is a complicated function of location and time which can only be obtained accurately from knowledge of the pre-collapse structure of the star, but limits may be placed upon $\dot{m}$ for the existence of the neutrinosphere well outside the Schwartzschild radius . Equation (15) restricts the accretion rate to values (for $r_\nu \gtrsim 3R_S$ say)

$$\dot{m}_{crit} \gtrsim 0.75\ M_\nu^{4/3}\ M_\odot\ s^{-1} \tag{18}$$

when standard values $n \sim 2.2$ and $f \sim 0.1$ are assumed. Certainly equations (15) - (17) should not be used for accretion rates smaller than this value. The high values of ρ, T, and L implied are never achieved because before reaching a temperature of 10

MeV, for example, cooling occurs in a fraction of a dynamic time scale (see Fig. 9) and the energy equation (eq. 14) which ignores sinks other than internal and kinetic energies, is violated. Equation (18) is useful, however, for indicating the accretion rate necessary to produce efficient, high energy neutrino emission. For example, in a 25 $M_\odot$ presupernova star (Weaver, Zimmerman, and Woosley 1978) the carbon, neon, oxygen and silicon shells have a density ranging from 10^5 to 10^8 g cm^{-3} and comprise a mass of $\sim$6 $M_\odot$. Using the free fall time scale (eq. 11) as a limit to how fast this material could be accreted gives an effective mass flux $\gtrsim$10 $M_\odot$ s^{-1}, so that a neutrinosphere would exist for the accretion of these layers. The helium shell, on the other hand, with density $\sim 10^3$ g cm^{-3}, however, and certainly the hydrogen shell with density $\sim 10^{-8}$ g cm^{-3}, would fall in at such a slow rate that there would be no neutrinosphere external to the event horizon. True, *some* emission will occur even though the gas is optically thin to neutrinos and the entropy of the envelope, S/k about 40, is not dissimilar to that of the very massive stars discussed above. But the collapse of these outlying regions will proceed very *non-homologously*. Thus density will scale as r^{-n} with $n < 3$. For our massive stars typically $n \sim 2.2$. With this scaling, falling from a radius of $\sim 10^{13}$ cm to $\sim 10^7$ cm, the density only rises to $\sim 10^5$ g cm^{-3} near the event horizon. As Figure 9 shows, isentropic compression to this density would give neither high temperature (hence no hard antineutrinos) nor efficient emission on a free fall time scale. Neglecting rotation, the matter just streams into the black hole with little dissipation. Similar arguments preclude substantial hard neutrino emission from black holes, massive or supermassive, undergoing *optically thick* (to light) accretion at any reasonable rate. Optically thin accretion and the presence of a shock might alter this conclusion.

From the above discussion we see how the accretion rate as a function of time might be approximated if the precollapse structure is known. Essentially $\dot{m}(\tau_{ff}) \sim \Delta M(\rho)/\tau_{ff}$ where $\Delta M(\rho)$ is that region of the star characterized by density ρ as the collapse begins and τ_{ff} is the free fall time scale (eq. 11) which should be divided by a factor $f^{1/2}$ if the collapse is not pressure free. It remains to estimate the value of $\dot{m}$ to be employed in equations (15) - (17) for very massive stars.

Considering only the pair instability case, the central density at the time that the collapse begins to be non-homologous is $\rho_i(0) \sim 10^7$ g cm^{-3}. There will be considerable variation about this number owing to the complicating effects of nuclear burning and the existence of *two* instabilities, the pair and the photodisintegration instabilities. Still, we may take the $n = 3$ polytrope calculated at this central density (plus or minus a factor of 10) as the starting model for the collapse. For the inner half of the mass of an $n = 3$ polytrope the quantity ρr^3 is initially given to a factor of two by the constant density approximation, *i.e.*, $M(r) \sim 4\pi/3 r_i^3 \rho_i(0)$. If we restrict our attention to only this portion of the matter and assume that during the collapse

ρ scales as r^{-n} with $n < 3$, then for the collapsing material

$$\rho(r) = (\frac{3M(r)}{4\pi})^{n/3} \rho_i^{1-n/3} r^{-n}. \tag{19}$$

Using this expression in the definition $\dot{m}(r) = 4\pi r^2 \rho(r) v(r)$ and evaluating at the neutrinosphere with $n = 2.2$ and $f = 0.1$ gives

$$\dot{m}_\nu = 21\ M_\nu^{5/6}\ M_\odot\ s^{-1}. \tag{20}$$

Since n is in fact time and space varying this is to be regarded as a *very approximate* expression. Combining this with equation (17) gives an *instantaneous* efficiency, in units of rest mass energy, for those cases where a neutrinosphere exists of

$$\begin{aligned} q(t) &= \frac{L_\nu}{\dot{m}_\nu c^2} \\ &\sim 0.005\ M_\nu^{3/14}, \end{aligned} \tag{21}$$

a value that is only weakly dependent upon the mass interior to the neutrinosphere. If the luminosity and accretion rate remain constant in time (not true in the general case) then $q(t) = Q_{rem}$ as defined in equation (5). Otherwise the two quantities are distinct as Q_{rem} is the ratio of the *integrals* over all time of the numerator and denominator in equation (21)

The values obtained using equations (15) - (21) compare favorably with those found in the numerical models (§2*c*) while a neutrinosphere exists. For example, in the collapsing 150 $M_\odot$ helium star when the mass interior to the neutrinosphere has reached 12 $M_\odot$ one has from the computer $r_\nu = 2.5 \times 10^7$ cm, $T_\nu = 4.0$ MeV, $\rho_\nu = 5 \times 10^9$ g cm^{-3}, $L_\nu = 2 \times 10^{54}$ erg s^{-1} (in electron antineutrinos), and $\dot{m} = 180$ $M_\odot$ s^{-1} implying an instantaneous efficiency $q = (L_\nu / \dot{m} c^2)$ of 0.9%. Equations (15) through (21), on the other hand imply $r_\nu = 6.9 \times 10^7$ cm, $T_\nu = 3.5$ MeV, $\rho_\nu = 2.8 \times 10^9$ g cm^{-3}, $L_\nu = 4.1 \times 10^{54}$ erg s^{-1}, $\dot{m} = 160$ $M_\odot$ s^{-1}, and $q = 0.8\%$ when typical values $f \sim 0.1$ and $n \sim 2.2$ are employed.

We emphasize again that these equations remain valid only so long as significant optical depth remains outside the event horizon. Once this condition is violated the efficiency declines rapidly. As Figure 9 shows, it is difficult to attain dynamical temperatures greater than ~4 MeV, which is near the effective temperature of the neutrinosphere when one exists. Yet the sharp rise of density and temperature near the black hole imply that these extreme conditions can exist in, at most, a very small volume. *Hence blackbody emission at ~4 MeV is an upper bound to the emission achieved in any (optically thick) circumstances.* The rapidly increasing gravitational red shift also acts to curtail the volume emission. Our calculations show (Fig. 6) that

shortly after the neutrinosphere is "eaten" the efficiency for antineutrino emission becomes trivial. Thus the eventual accretion of the entire collapsing object implies a much smaller total Q_{rem}.

e. *The Collapse of Supermassive Stars ($M \gtrsim 10^5\ M_\odot$)*

The general relativistic instability of stars attempting to ignite hydrogen burning on the main sequence with mass in excess of $\sim 10^5\ M_\odot$ has been realized for some time (Iben 1963; Fowler 1966; Fricke 1973, 1974). Recent numerical studies by Fuller, Woosley, and Weaver (1983,1985) have provided detailed results from a numerical study of a grid of masses from 10^5 to $10^6\ M_\odot$ and metallicities from zero to 0.02. As a representative case we calculate here the neutrino emission from a $5 \times 10^5\ M_\odot$ model with zero initial metallicity (75% hydrogen and 25% helium by mass) that collapses to a black hole. For details of the precollapse evolution and instability see Fuller *et al.* The entropy of the initial model when the central temperature has first reached $\sim$1 MeV, is close to 200, a substantially larger value than in the 150 and 500 $M_\odot$ helium cores considered in the previous subsection. Consequently higher temperatures are obtained at lower density and pair neutrino emission and absorption processes are more important (Fig. 8). Also, owing to the fact that the trapped surface forms at a considerably lower density, $\rho_{BH} \sim (3c^6)/(32\pi G^3 M^2) = 1.8 \times 10^6 (10^5\ M_\odot/M)^2\ \mathrm{g\ cm^{-3}}$, the high emission temperatures and even existence of a well defined neutrinosphere are circumvented (see Fig. 9), *i.e.*, all of the emission occurs in plasma that is "optically thin" to neutrinos.

Following the supermassive star through the point where a trapped surface forms is accomplished approximately using the Wilson-Bowers neutrino transport code which contains post Newtonian corrections to gravity (but which is not in itself fully general relativistic). The unstable collapsing star is adapted from the Fuller *et al.* model at a time when the central temperature has reached 5×10^9 K which corresponds to a central density $\rho = 5.5 \times 10^4\ \mathrm{g\ cm^{-3}}$. The combined neutrino and antineutrino luminosity at this point was $7.9 \times 10^{54}\ \mathrm{erg\ s^{-1}}$, owing chiefly to pair annihilation, and the peak collapse velocity was $7 \times 10^9\ \mathrm{cm\ s^{-1}}$ at the edge of the homologously collapsing core which included $2.2 \times 10^5\ M_\odot$. Trapped surface formation is said to occur when the mass interior to any given radius exceeds the Swartzchild value, $M(R) = Rc^2/(2G)$. Relativistic redshifts are applied to the neutrinos emitted external to this surface. The results of this calculation are displayed in Figures 10 and 1 and in Table 1. The collapse is quite non-homolgous, as Fuller *et al.* have previously described, and consequently the trapped surface initially forms deep within the core at $\sim 1.1 \times 10^5\ M_\odot$, or about 20% of the star. The temperature never rises to much more than 2 MeV outside the event horizon and a neutrinosphere never forms. Soon the black hole consumes most of the hot dense matter that might have been efficient in the emission of neutrinos.

Following that, the rest of the star just accretes into the hole with very little emission. The overall efficiency is only $Q_{rem} = 2.9 \times 10^{-4}$ Mc^2 and the total energy output in electron antineutrinos, 2.6×10^{56} erg with average energy 1.9 MeV.

III. DISCUSSION

A variety of gravitational collapses have been discussed in this paper: supernovae producing neutron stars, "failed" supernovae producing black holes, and the direct collapse of very massive and supermassive stars into black holes. We have been careful to differentiate antineutrino fluxes that *must* exist (eq. 1), from those that *probably* exist, but which have large red shifts (eq. 3), and those that *could* exist (eq. 5), also with large redshifts. The signal associated with present day supernovae (eq. 1) is very small and, as we shall see, well below the limit of detectability. The flux of antineutrinos associated with the formation of "dark matter," on the other hand (eq. 5), is numerically much larger but is unfortunately characterized by a softer spectrum, a condition that is exacerbated by the cosmological redshift. Indeed, for each range of stellar masses, one is confronted with limits that suggest that the actual signal, which depends sensitively on average antineutrino energy as well as flux, is not likely to be detectable in the near future.

For stars in the mass range 8 to 100 $M_\odot$, both the efficiency, $Q_{rem} \sim 2\%$, and the initial spectral hardness, $\langle \epsilon_\nu \rangle \sim 14$ MeV, are relatively large favoring the production of antineutrinos that might be visible above the terrestrial background. Unfortunately the nucleosyntheic limits (eq. 4 and Fig. 6 of Carr, Bond, and Arnett 1984) are so restrictive that neutron star remnants from this mass range could constitute no more than $\Omega \lesssim 10^{-3}$ in equation (5). Hence the background from this mass range is probably no more than a few 100 cm^{-2} s^{-1}. This restriction could be circumvented if *most* stars in this mass range experienced failed core bounces and collapsed to black holes with no nucleosynthetic ejection. However, given that at least a fraction of these stars, probably those with the lowest mass and hence greatest abundance, must explode in order to explain the existence of neutron stars and given the possibility that rotational effects may lead to mass ejection even if the core bounce fails (Bodenheimer and Woosley 1983), this hedge must be regarded as an unlikely one.

Stars in the 100 to 300 $M_\odot$ range explode with negligible hard antineutrino production. Stars in the 300 to 1000 $M_\odot$ range, typified by the 150 and 500 $M_\odot$ helium cores studied in §2*c*, collapse to black holes that *could* (Carr, Bond, and Arnett 1984) constitute as much as 10% of the closure density of the universe. However, the antineutrino spectrum is softer (Fig. 1, Table 1), $\langle \epsilon_\nu \rangle \sim 5$ MeV$/(1 + z_f)$, and the efficiency per remnant mass lower, by about a factor of 10, than those Type II supernovae that leave neutron stars. Especially given that redshifts $z_f \gtrsim 3$ are likely to characterize the epoch when substantial mass might have formed into such stars,

the antineutrinos produced by very massive stars will be too soft to detect above the terrestrial background. The flux, given by equation 5, would be a few hundred antineutrinos cm^{-2} s^{-1} at an energy that might typically be an MeV or so.

For truly supermassive stars, $M \gtrsim 10^5$ $M_\odot$, the efficiency is low (§2*e*) and the neutrinos are certainly too soft to be seen above the huge terrestrial background (*e.g.*, $\phi \sim 10^5$ cm^{-2} s^{-1} at 2 MeV from the decay of bismuth and lead isotopes; $\phi \sim 10^6$ cm^{-2} s^{-1} at 1 MeV from the decay of ^{40}K; Krauss, Glashow, and Schramm 1984). Typical antineutrino energies from supermassive stars would likely have energy, once redshifted to the era of galaxy formation, of less than 1 MeV.

Thus, all things considered, the strongest *detectable* signal is likely to originate from Type II supernovae in the 8 to 100 $M_\odot$ range occurring during the era of galaxy formation. Taking equation (4) as an estimate of the flux and a redshift $z_f \sim 1$ (*i.e.* $(1 + z_f) \sim 2$) one can consider the plausibility of detection. This redshift is quite uncertain but probably a lower bound since it would correspond to a peak of star formation in an Einstein deSitter Universe at an age of about 4 billion years (for $H_o \sim 55$ km s^{-1} Mpc^{-1} which implies a present age of ~12 billion years). Present data (Djorgovski and Spinrad 1984) may be more consistent with z_f for peak star formation ~ 3 to 5. For illustration we adopt the optimistic value. For a detector consisting of one metric kiloton (10^9 g) of hydrogen-rich liquid scintillator and taking a composition, for example, of liquid methane (Barabash *et al.* 1981; Chen 1982; Cline 1984), a flux of 250 antineutrinos cm^{-2} s^{-1}, each with characteristic energy 7 MeV, would produce a reaction rate (eq. 8) of 1.6×10^{-7} s^{-1}. Thus a counting rate of roughly 5 events per year would be expected. Since detectors as large as 10 kilotons and greater are currently contemplated for future experiments to search for proton decay (Cline 1984), a counting rate of perhaps one per week might be realized.

By any standards this is a very small number. However, one is not dealing with the extraction of single atoms from multi-ton detectors as in the case of the solar neutrino experiment, but with the actual detection, real time, of individual events. The fundamental property of liquid scintillator that makes it desirable as a nucleon decay detection medium is its ability to convert the kinetic energy of charged particles to visible photons. For all but heavily ionizing particles the scintillation response is linearly related to the energy deposited. Since the energy needed to produce each optical photon is about 200 eV and collection efficiencies of 2% and photoelectron conversion of 10% are easily achieveable (Cherry *et al.* 1982a), an energy deposition of 7 MeV (the neutron presumably would give up its energy to a recoil proton) would produce ~70 photoelectrons and allow about 10% energy resolution.

Of greater concern than the energy resolution, however, is the background inherent in such a measurement. It is hoped that competing physical events will occur at a slow rate or can be supressed. Neutrinos produced by cosmic ray air showers, for example, have a very low flux and can be discriminated against on the basis of their

high energy (Cherry *et al.* 1982a). The muon background from cosmic rays is very large on the surface of the Earth but declines greatly in the deep mines where proposed proton decay experiments are to be situated. It is expected that all muon events can be rejected (Cherry *et al.* 1982a). Additional discrimination may be available, at a price, by looking for positrons *in coincidence with neutrons* (Phillips *et al.* 1984 although the neutrinos we seek are ~5 times less energetic than considered in their paper). Also the efficiency for such a joint detection, estimated by Phillips *et al.* to be ~6%, may be unacceptably small. Of grave concern is the large background from random counts in the photomultiplier tubes (*cf.* Burrows 1984). We do not know if this restriction (*e.g.* 2×10^6 counts s^{-1} in an 8 kiloton water detector) can be circumvented by anti-coincidence discrimination or other techniques. Compton scattering in the detector of γ-rays produced by the radioactive decay of terrestrial atoms may also constitute a severe background problem, especially at the low neutrino energies of interest here.

Perhaps the best one can say is that the possible detection of the antineutrino background discussed here should provide "food for thought" for those engaged in the design of large proton decay experiments. It should be kept in mind, however, that the "guaranteed" flux, equation (1), is orders of magnitude less even than the 250 cm^{-2} s^{-1} employed in the above example, and the era of galaxy formation and nucleosynthesis may easily be moved back to $z_f >> 2$, in which case the liklihood of seeing anything is extremely small. On the other hand, the flux from the occasional *galactic* supernova, Type II, is much larger (*cf.* Cherry *et al.* 1982b; Burrows 1984) and should be (comparatively) easily detectable.

It is also of some interest, if only academic, to consider the contribution of this neutrino background to the mass of the universe (Bisnovatyi-Kogan and Seidov 1984). A flux of 250 antineutrinos cm^{-2} s^{-1} each with energy 7 MeV would give a "density" of $\sim 10^{-34}$ g cm^{-3}, or about 5 times less than in the (microwave) photon background. This is just the mass in electron antineutrinos and the mass in all six varieties of neutrinos would be (about 6 times) larger. Thus the total mass energy density in the neutrino background from gravitational collapse is just comparable to that in the observed background radiation. The impact of the ordinary electron neutrinos on the solar neutrino experiment would be negligible (Bisnovatyi-Kogan and Seidov 1984).

Finally it has been speculated (Domogatsky and Nadyozhin 1977; Woosley 1977) that the large flux of neutrinos and antineutrinos produced by gravitational collapse in the core may induce nuclear transmutation in the envelope of the star which, if ejected, might be of nucleosynthetic import. Woosley (1977) and Domogatsky, Nadyozhin, and Eramzhyan (1977), in particular, have suggested the synthesis of deuterium by $p(\bar{\nu}_e, e^+)n(p,\gamma)^2H$ in the hydrogen-rich enevelope of the star. Typically the deuterium production relative to hydrogen is $P \sim 7 \times 10^{-6}$ $(10^{10}\ cm/R)^2$, where R is the distance from the imploding core and an explosion of 10^{52} erg producing 15 MeV electron antineutrinos is assumed. Since one must go to radii of several times 10^{12}

cm in order both to encompass a fraction of the hydrogen envelope of a massive star and get to low enough temperatures that the deuterium does not burn, production by this mechanism in massive and very massive stars is negligible. For the supermassive star considered here (Table 1), the production ratio at 5×10^{12} cm, where the pre-collapse conditions would allow the survival of substantial deuterium, would be about 10^{-8}. Obviously this is too small to be of cosmic import. Also, the supermassive stars considered by Fuller, Woosley, and Weaver (1985) either explode (those with near solar metallicity) and do not attain high central temperatures or produce much antineutrino flux, or collapse entirely, hence ejecting no nucleosynthesis. These results may be an artifact of a one-dimensional calculation and might be altered when future studies include rotation. Mass bifurcation, *i.e.*, collapse *and* explosion, is a possibility (*cf.* Bodenheimer and Woosley 1983). If future calculations show this occurring in *any* of the models studied here, neutrino-induced nucleosynthesis, especially of rarer species, ^{6,7}Li, ^{9}Be, ^{10,11}B, as suggested by Domogatsky, Nadyozhin, and Eramzhyan (1977), might be reconsidered.

This paper was begun following conversations with David Cline at the Aspen Center for Physics during the summer of 1984. Cline pointed out the feasiblity of detecting a signal from supernovae (as discussed in a preprint by Krauss, Glashow, and Schramm) and suggested that more accurate calculations would be desirable before considering the utility of such a search. Conversations with other attendees at the Aspen center workshop on supernovae, especially Adam Burrows and Amos Yahil, were also stimulating and some of the concepts developed in this paper, *e.g.* equation (5), were the product of our joint work. We also appreciate a critical reading of the manuscript by Burrows. This work has been supported by the National Science Foundation (AST 81-08509) and, at Livermore, by the U. S. Department of Energy through contract number W-7405-ENG-48 and the Institute for Geophysics and Planetary Physics (IGPP).

REFERENCES

Axelrod, T. S. 1980, Ph.D. thesis UCSC, available as UCRL preprint 52994 from Lawrence Livermore National Laboratory.

Barkat, Z., Rakavy, G., and Sack, N. 1967, *Phys. Rev. Lettr.*, **18**, 379.

Barabash, A. S. *et al.* 1981,*Nuclear Instruments and Methods*, **186**, 525.

Bisnovatyi-Kogan, G. S., and Seidov, Z. F. 1984, *Ann. N.Y. Acad Sci.*, **422**, 319.

Bodenheimer, P. B., and Woosley, S. E. 1983, *Ap. J.*, **269**, 281.

Bond, J. R., Arnett, W. D., and Carr, B. J. 1982, in *Supernovae: A Survey of Current Research*, ed. M. J. Rees and R. J. Stoneham, (D. Reidel: Dordrecht), p. 303.

_____. 1984, *Ap. J.*, **280**, 825.

Bowers, R. L., and Wilson, J. R. 1982a, *Ap. J.*, **263**, 366.

_____. 1982b, *Ap. J. Suppl.*, **50**, 115.

Brown, G. E., Baym, G., and Bethe, H. A. 1982, *Nucl. Phys. A*, **375**, 481.

Burrows, A. 1984, *Ap. J.*, **283**, 848.

_____. 1985, preprint "Speculations on the Fizzled Collapse of a Massive Star," State University of New York, Stony Brook.

Carr, B. J., Bond, J. R., and Arnett, W. D. 1984, *Ap. J.*, **277**, 445.

Chen, H. H. 1982, in *Proceedings of the 1982 Summer Workshop on Proton Decay Experiments*, Argonne National Lab. reprint ANL-HEP-PR-82-24, ed. D. S. Ayres, p. 274.

Cherry, M. L., Davidson, I., Lande, K., Lee, C. K., Marshall, E., Steinberg, R. I., Cleveland, B., Davis, R., and Lowenstein, D. 1982a, in *Proceedings of the 1982 Summer Workshop on Proton Decay Experiments*, Argonne National Lab. reprint ANL-HEP-PR-82-24, ed. D. S. Ayres, p. 150.

Cherry, M. L., Davidson, I., Lande, K., Lee, C. K., Marshall, E., and Steinberg, R. I. 1982b, in *Proceedings of the 1982 Summer Workshop on Proton Decay Experiments*, Argonne National Lab. reprint ANL-HEP-PR-82-24, ed. D. S. Ayres, p. 300.

Cline, D. 1984, private communication.

Colgate, S. A., and McKee, C. 1969, *Ap. J.*, **157**, 623.

Dar, A. 1984, Technion preprint PH-84-54, Technion-Israel Institute of Technology.

Domogatsky, G. V., and Nadyozhin, D. K. 1977, *MNRAS*, **178**, 33.

Domogatsky, G. V., Nadyozhin, D. K., and Eramzhyan, R. A. 1977, preprint, "The Production of the Light Elements Due To Neutrinos Emitted By Collapsing Stellar Cores," *Inst. Applied Math. No. 43*, Acad. Sci. USSR, Moscow.

Doroshkevich, A. G., Khlopov, M. Yu, Sunyaev, R. A., Szalay, A. S., and Zeldovich, Ya. B. 1981, *Ann. N.Y. Acad. Sci.*, **375**, 32.

Djorgovski, S., and Spinrad H. 1985, preprint. submitted to *Ap. J.*

Fowler, W. A. 1966, in *High Energy Astrophysics*, ed. L. Gratton, (Academic Press: New York), p. 313.

Fowler, W. A., and Vogl, J. L. 1964, in *Lectures in Theoretical Physics, Volume VI*, (University of Colorado Press: Boulder), p. 379.

Fricke, K. J. 1973, *Ap. J.*, **183**, 941. _____. 1974, *Ap. J.*, **189**, 535.

Fuller, G. M., Fowler, W. A., and Newman, M. J. 1982a, *Ap. J. Suppl.*, **48**, 279.

_____. 1982b, *Ap. J.*, **252**, 715.

_____. 1985, submitted to *Ap. J.*

Fuller, G. M., Woosley, S. E., and Weaver, T. A. 1983, *B.A.A.S.*, **14**, 956.

_____. 1985, submitted to *Ap. J.*

Gordon, M. A., and Burton, W. B. 1976, *Ap. J.*, **208**, 346.

Hillebrandt, W. 1984, *Ann. N.Y. Acad. Sci.*, **422**, 197.

Hillebrandt, W., and Muller, E. 1984, preprint "Neutrinos from Collapsing Stars," Max Planch Inst., Garching.

Iben, I. 1963, *Ap. J.*, **138**, 1090.

Krauss, L. M. Glashow, S. L., and Schramm, D. N. 1984, *Nature*, **310**, 191.

Michel, F. C. 1972, *Ap. and Spac. Sci.*, **15**, 153.

Miller, G. E. and Scalo, J. M. 1979, *Ap. J. Suppl.*, **41**, 513.

Nadezhin, D. K., and Ostroshenko, I. V. 1980, *Astron. Zh.*, **57**, 78.

Nomoto, K. 1984, in *Stellar Nucleosynthesis*, ed C. Chiosi and A. Renzini, (D. Reidel:Dordrecht), p. 239.

Nomoto, K., Thielemann, F. K., and Yokoi, K. 1984, *Ap. J.*, **286**, 644.

Palla, F., Salpeter, E. E., and Stahler, S. W. 1983, *Ap. J.*, **271**, 632,

Phillips, G. C. *et al.* 1984, *Nuclear Instruments and Methods*, **221**, 334.

Scalo, J. M. 1984, preprint "The Evidence for Universality of the Large Scale Initial Mass Function," University of Texas.

Silk, J. 1977, *Ap. J.*, **211**, 638.

Tammann, G. A. 1982, in *Supernovae: A Survey of Current Research*, ed. M. J. Rees and R. J. Stoneham, (D. Reidel: Dordrecht), p. 371.

Tubbs, D. L., and Schramm, D. N. 1975, *Ap. J.*, **201**, 467.

Weaver, T. A., and Woosley, S. E. 1980, *Ann. N.Y. Acad. Sci.*, **336**, 335.

Weaver, T. A., Zimmerman, G . B., and Woosley, S. E., 1978, *Ap. J.*, **225**, 1021.

Whelan, J., and Iben, I. 1973, *Ap. J.*, **186**, 1007.

White, S. M., and Rees, M. J. 1981, *Ann. N.Y. Acad. Sci.*, **375**, 32.

Wilson, J. R. 1984 in *Numerical Astrophysics*, ed. J. Centrella, J. LeBlanc, and R. Bowers, (Jones and Bartless: Boston), in press.

Wilson, J. R., Mayle, R., Woosley, S. E., and Weaver, T. A. 1985, in *Proc. Twelfth Texas Symp. on Rel. Ap.*, to be published by *Ann. N. Y. Acad. Sci.*

Woosley, S. E. 1977, *Nature*, **269**, 42.

Woosley, S. E., and Weaver, T. A. 1982, in *Supernovae: A Survey of Current Research*, ed. M. J. Rees and R. J. Stoneham, (D. Reidel: Dordrecht), p. 79.

Woosley, S. E., Axelrod, T. S., and Weaver, T. A. 1984, in *Stellar Nucleosynthesis*, ed. C. Chiosi and A. Renzini, (D. Reidel: Dordrecht), p. 263.

Yahil, A. 1984, in *Stellar Nucleosynthesis*, ed. C. Chiosi and A. Renzini, (D. Reidel: Dordrecht), p. 251.

Yahil, A., Sandage, A., and Tammann, G. A. 1980, *Ap. J.*, **242**, 448.

Figure Captions

FIG. 1.- Time integrated antineutrino spectra from six stars that have undergone gravitational collapse. In all cases the spectra have been integrated until essentially all neutrino emission had ceased. The quantity $\frac{dE}{M d\epsilon}\, d\epsilon$ is the total energy emitted in the form of electron antineutrinos having individual energies between ϵ and $\epsilon + d\epsilon$ divided by the total stellar mass in solar mass units. The area under each curve multiplied by the mass of the star in solar masses is thus the total electron antineutrino energy emitted during the event. The 10, 15, and 25 $M_\odot$ stars produce supernovae with neutron star remnants. The 150, 500, and 5×10^5 $M_\odot$ stars collapse to black holes. Since the code used to calculate these spectra does not include the gravitational redshift (except for the 5×10^5 $M_\odot$ star), the curves shown have been renormalized by the amounts shown in Table 1.

FIG. 2. - Physical variables and composition of the 150 and 500 $M_\odot$ stars used as initial data for the collapse code (Woosley and Weaver 1984, unpublished). Variables are depicted at a time in each model when the central temperature has reached approximately 1 MeV. The temperature (T), density (ρ), and collapse velocity (v) are given in cgs units with subscripts to indicate the appropriate multiplicative power of 10. Approximate elemental composition is indicated at the base of each figure. Here "Fe" denotes all species in the iron group and, at this point, is chiefly the isotope ^{56}Ni. The complex shape of the collapse velocity profiles, especially in the 150 $M_\odot$ model, is a consequence of the partial recovery of hydrostatic equilibrium in the core following the pair instability but prior to the photodisintegration instability.

FIG. 3. - Constant mass trajectories (identified by the enclosed mass in solar units) for the 500 $M_\odot$ star as it collapses to a black hole. Only the inner 400 $M_\odot$ is shown in the figure. Trajectories end on a curve determined by the condition that $r = 4GM/c^2$. The dashed line represents the position of the neutrinosphere and the

time origin is arbitrarily placed near the time a black hole forms.

FIG. 4. - Time integrated antineutrino spectra for the 150 $M_\odot$ star sampled at several times. Time $t_1 = 0$ corresponds to the first appearance of the neutrinosphere. At time t_3 the neutrinosphere vanishes as it is drawn into the trapped surface. This corresponds closely to the final spectrum (see Fig. 1). The times are chosen so that roughly equal amounts of total energy ($\sim 2 \times 10^{52}$ erg) are emitted between the two time intervals indicated. The spectra include a gravitational redshift.

FIG. 5. - Radiated antineutrino energy and time-integrated mass accretion rate as a function of time for the 150 and 500 $M_\odot$ models. The mass interior to the neutrinosphere is taken as the definition of $\int \dot{m} dt$, and is measured in solar mass units. The neutrinosphere moves into the trapped surface about 50 - 60 ms after its initial formation (t = 0 on the above graph) for both models. Energy is in units of 10^{52} erg. The asymptotic value of the total emitted energy (without redshift included) are 9.8×10^{52} erg and 1.40×10^{53} erg for the 150 and 500 $M_\odot$ stars respectively. See Table 1 for an estimate of the redshifted energy.

FIG. 6.- Electron antineutrino "light curves" showing luminosity and cumulative energy output ($E = \int L_\nu \, dt$) as functions of time in the 150 and 500 $M_\odot$ models. The arbitrary time axis has been shifted so that peak luminosity occurs for both stars at the same time and the indicated luminosity is edited in an optically thin region situtated at 3×10^8 cm for the 150 $M_\odot$ model and 10^9 cm for the 500 $M_\odot$ model. Observers farther out would see the same signal, but delayed by light travel time. Vertical bars denote the instant at which trapped surfaces are formed in the two models. The narrow range shown on the base of the time axis (0.06 s) is the interval when a region optically thick to neutrinos existed outside the event horizon in the 150 $M_\odot$ model. In the 500 $M_\odot$ model, a neutrinosphere forms almost simultaneously with the trapped surface. Even so, most of the energy in that model is emitted while

the optical depth remains near unity. Note also an effect of the finite speed of light. Neutrinos emitted as the trapped surface forms take ~0.05 s to travel to the fiducial point. The above curves have not been corrected for gravitational redshift.

FIG. 7. - Temperature and density of matter at the neutrinosphere and the neutrinosphere radius for the 150 and 500 $M_\odot$ models as a function of time. Time is measured from the formation of the neutrinosphere. All units are in *cgs* except for temperature which is in MeV. The jagged nature of the curves is an artifact of coarse zoning in the central regions where $\Delta r/r$ may be as great as 0.1.

FIG. 8. - Thermodynamic conditions characteristic of the collapse of very massive stars. All quantities have been evaluated for a plasma in nuclear statistical equilibrium and for having equal numbers of neutrons and protons. The cross-hatched region in the upper left corner indicates the nucleon-alpha phase transition. For the region of interest the composition will be predominantly nucleons, leptons, and photons. For regions above the line $3/4\eta\rho Y_e N_A kT = (1 + 3/4)aT^4$, where η is the chemical potential, electrons and positrons will be degenerate and for regions below the line $3/2\rho N_A kT = (1 + 7/4)aT^4$ the energy (and pressure) in nucleons will be negligible compared to that in the relativistic electrons and photons. For regions below the line $S_{nucleon} = S_\gamma + S_{pair}$ most of the *entropy* of the gas will be in the relativistic particles (see also Bond, Arnett, and Carr 1984) and for regions below the line $\dot{\epsilon}_{nucleon} = \dot{\epsilon}_{pair}$ electron neutrino losses from pair annihilation (eq. 13) will dominate over those from the capture of electrons and positrons on nucleons. For the most part, we are interested in a nucleon plasma where most of the energy is contained in non- degenerate relativistic particles with energy losses dominated by capture reactions.

FIG. 9. - Time scales and paths of constant total entropy for collapsing very massive stars. Lines of constant dimensionless entropy, 15 and 50, are shown. Stars in the (main sequence) mass range 300 to several thousand $M_\odot$ should evolve so as

to enter this diagram from the left within this band. Somewhere within the region given by cooling time scale (total internal energy divided by neutrino loss rate from capture and pair annihilation) equal to 0.2 to 1 times the local hydrodynamic time, τ_{HD}, collapsing material will begin to lose energy as fast as gravitational compression can supply it. The temperature ceases to increase and the evolutionary path turns upward. When the diffusion time, τ_{DIF}, for a characteristic region is comparable to the hydrodynamic time neutrinos will be trapped. Emission of neutrinos having characteristic temperature $\gtrsim$5 MeV is essentially impossible.

FIG. 10. - Time history of the electron antineutrino luminosity of a collapsing 5×10^5 $M_\odot$ star. The luminosity declines dramatically as the hot, dense, central regions of the star are enveloped by a black hole.

TABLE 1

ELECTRON ANTINEUTRINO EMISSION FROM STELLAR COLLAPSE

M ($M_\odot$)	M_{rem} ($M_\odot$)	$\int L_{\bar{\nu}} dt$[a] (10^{52} erg)	$T_{\bar{\nu}}$ (MeV)	$\langle \varepsilon_{\bar{\nu}} \rangle$ (MeV)	$Q_{tot}(\bar{\nu}_e)$ (%)	$Q_{rem}(\bar{\nu}_e)$ (%)	E/E_{code}
10	1.3	4.8	4.0	11	0.27	2.1	0.90
15	1.6	6.0	5.0	14	0.22	2.1	0.90
25	2.0	11	5.3	16	0.24	3.1	0.90
150	150	8.3	4.0	5.5	0.030	0.030	0.85
500	500	110	3.8	4.5	0.12	0.12	0.80
5×10^5	5×10^5	26,000	-	1.9	0.029	0.029	-

With the exception of the 5×10^5 $M_\odot$ model, the integrated energy has been redshifted by the amount shown in the last column since the collapse code does not take this into account. Q_{tot} and Q_{rem} are the ratios of emitted (electron antineutrino) energy to the rest mass of the total star and collapsed remnant respectively. The quantity $\langle \varepsilon_{\bar{\nu}} \rangle$ is the total energy divided by the number of neutrinos emitted.

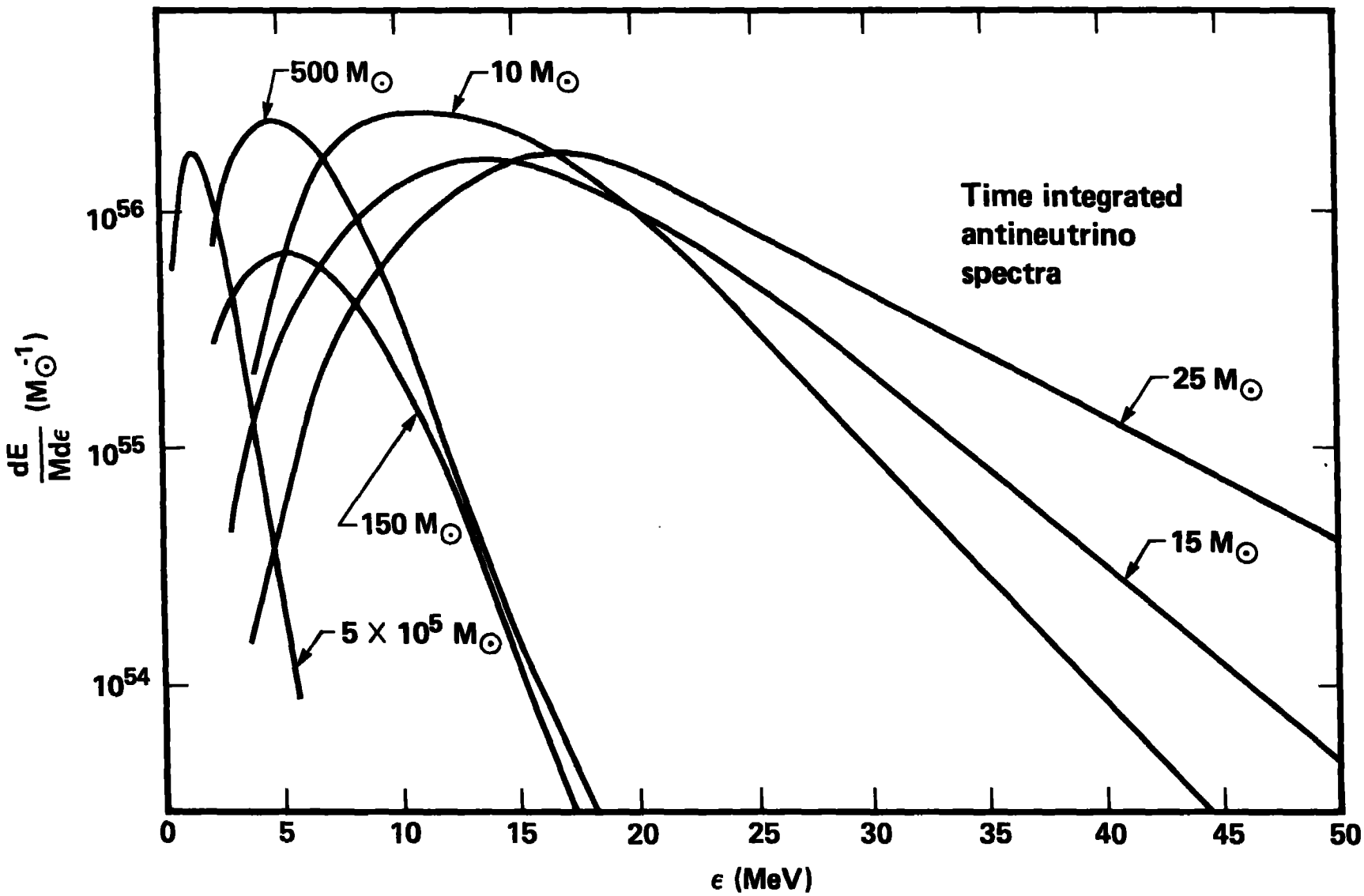
500 M⊙
10 M⊙
Time integrated
antineutrino
spectra
25 M⊙
15 M⊙
150 M⊙
5 × 10^5 M⊙
10^56
10^55
10^54
dE/Mdε (M⊙^-1)
0
5
10
15
20
25
30
35
40
45
50
ε (MeV)

FIGURE 1

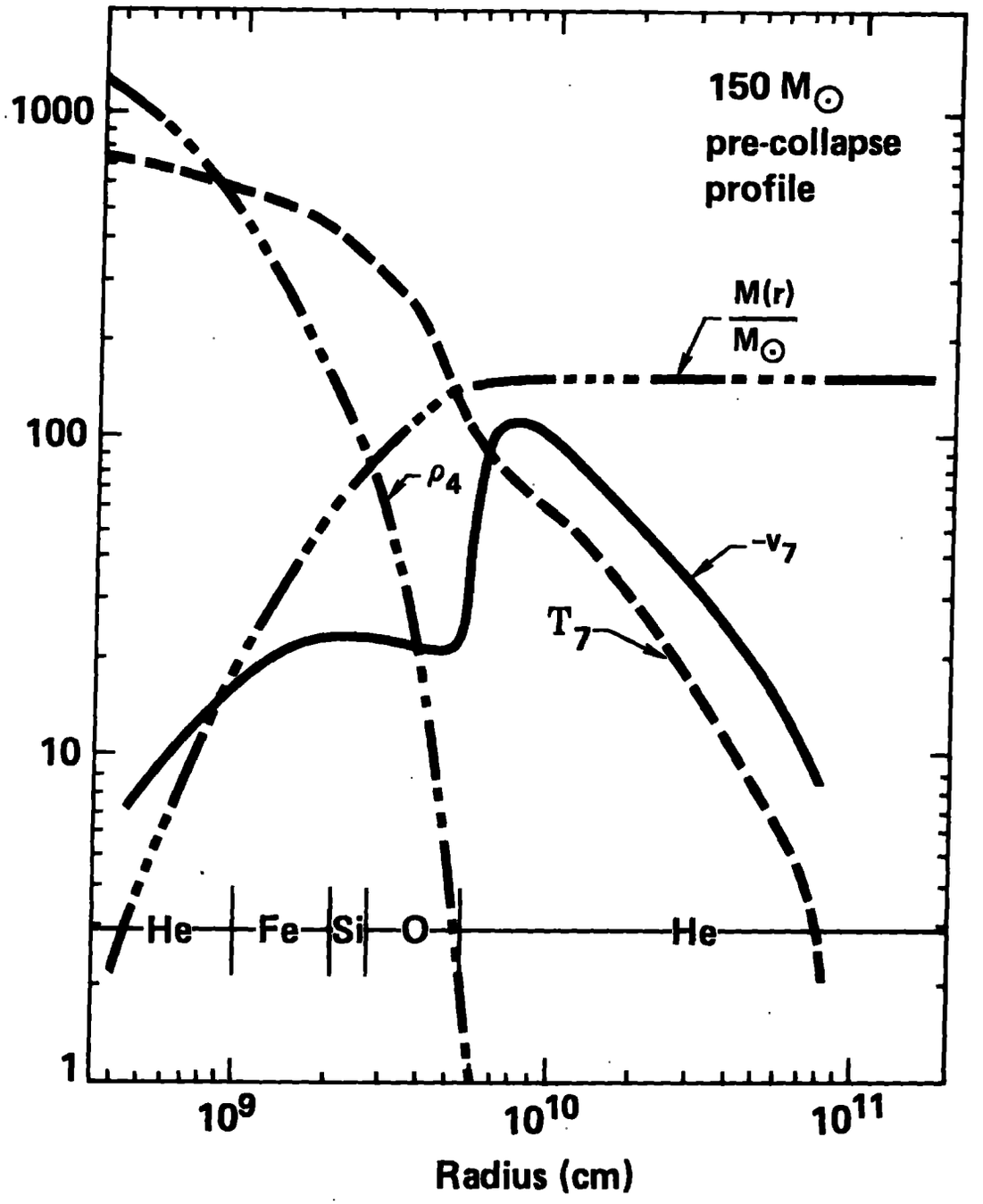
150 M⊙
pre-collapse
profile
M(r)/M⊙
ρ4
-v7
T7
1000
100
10
1
He
Fe
Si
O
He
10^9
10^10
10^11
Radius (cm)

FIGURE 2a

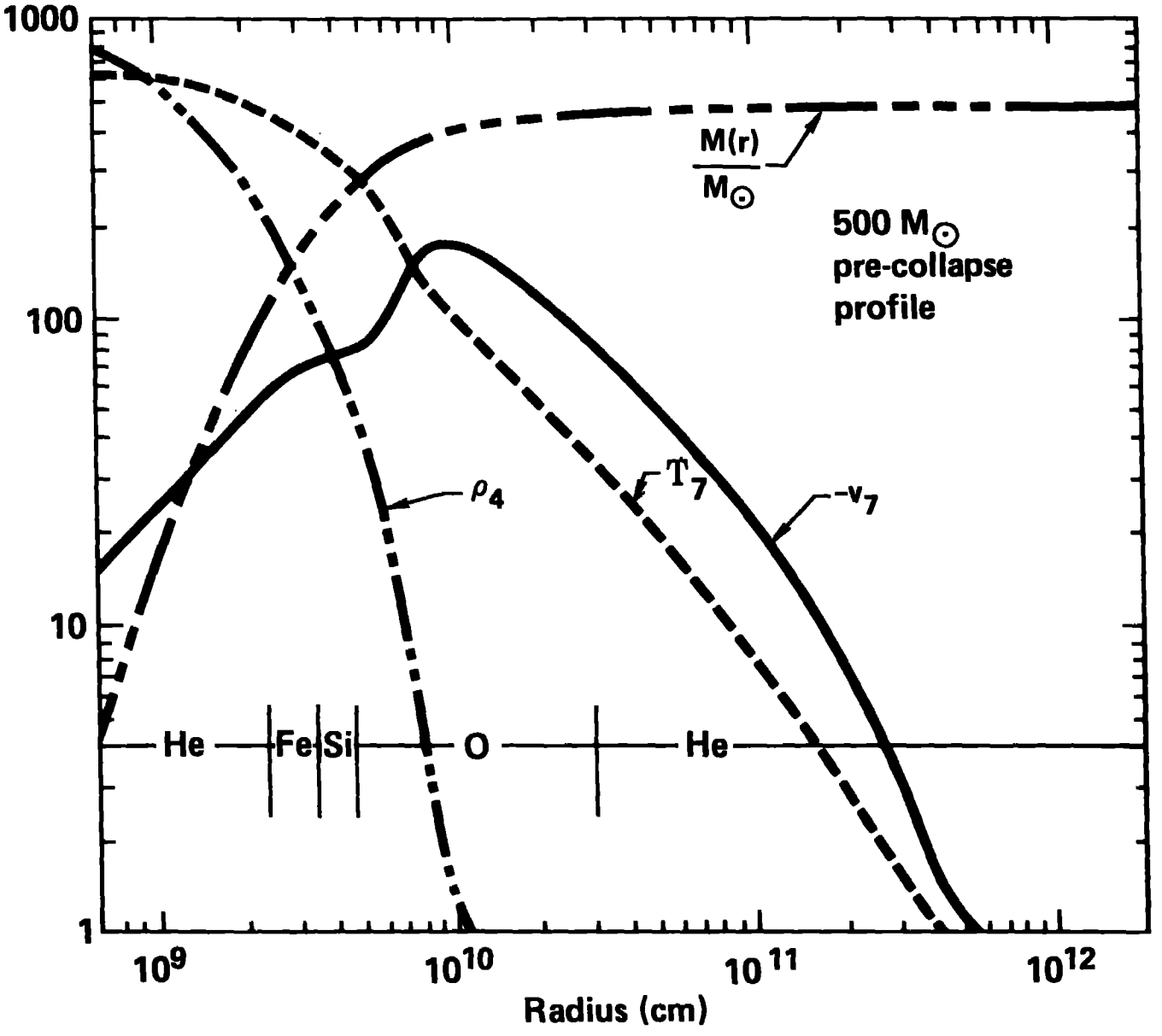
1000
100
10
1
M(r)
M⊙
500 M⊙
pre-collapse
profile
ρ4
T7
v7
He
Fe
Si
O
He
10^9
10^10
10^11
10^12
Radius (cm)

FIGURE 2b

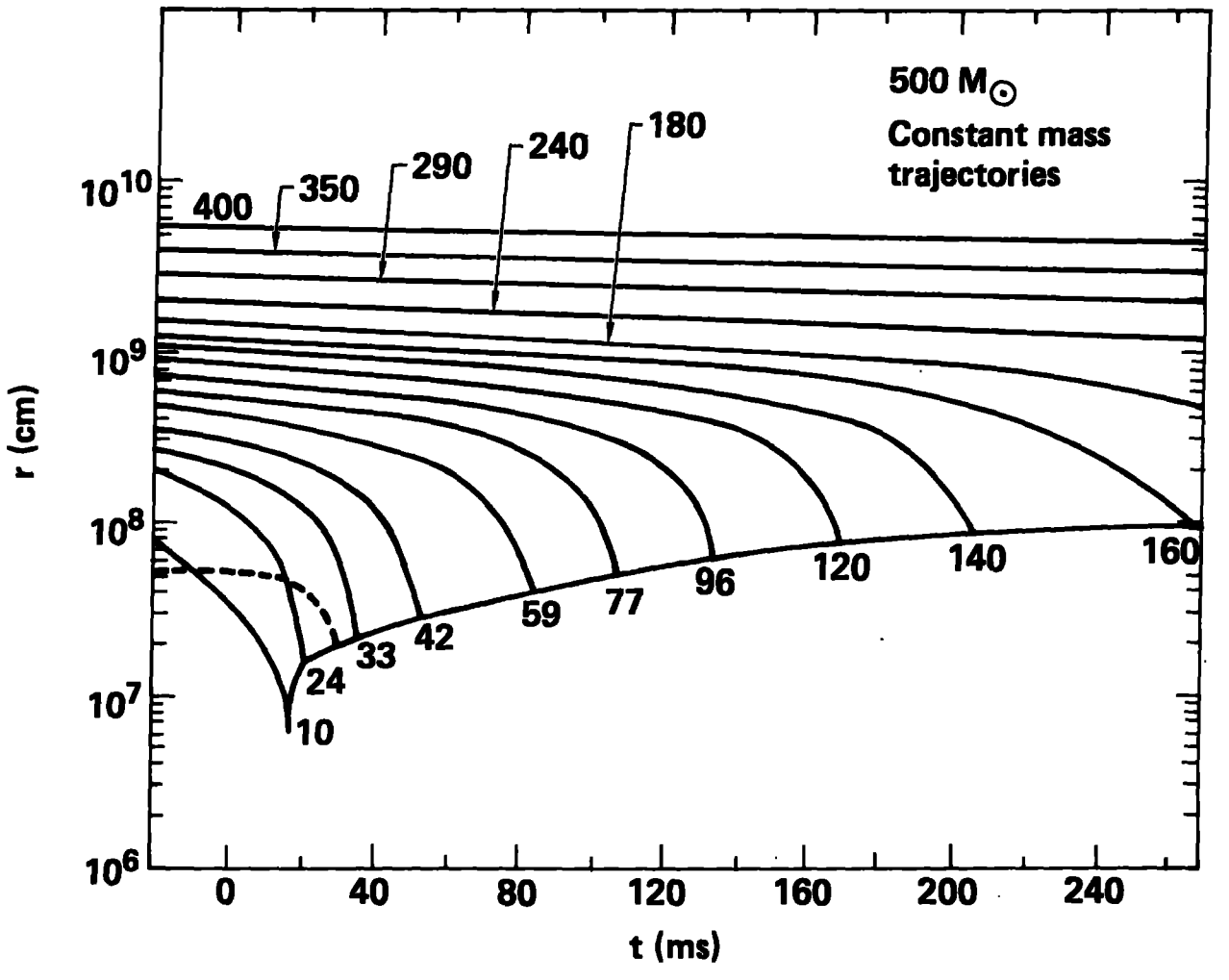
500 M⊙
Constant mass
trajectories
400
350
290
240
180
160
140
120
96
77
59
42
33
24
10
10^10
10^9
10^8
10^7
10^6
r (cm)
0
40
80
120
160
200
240
t (ms)

FIGURE 3

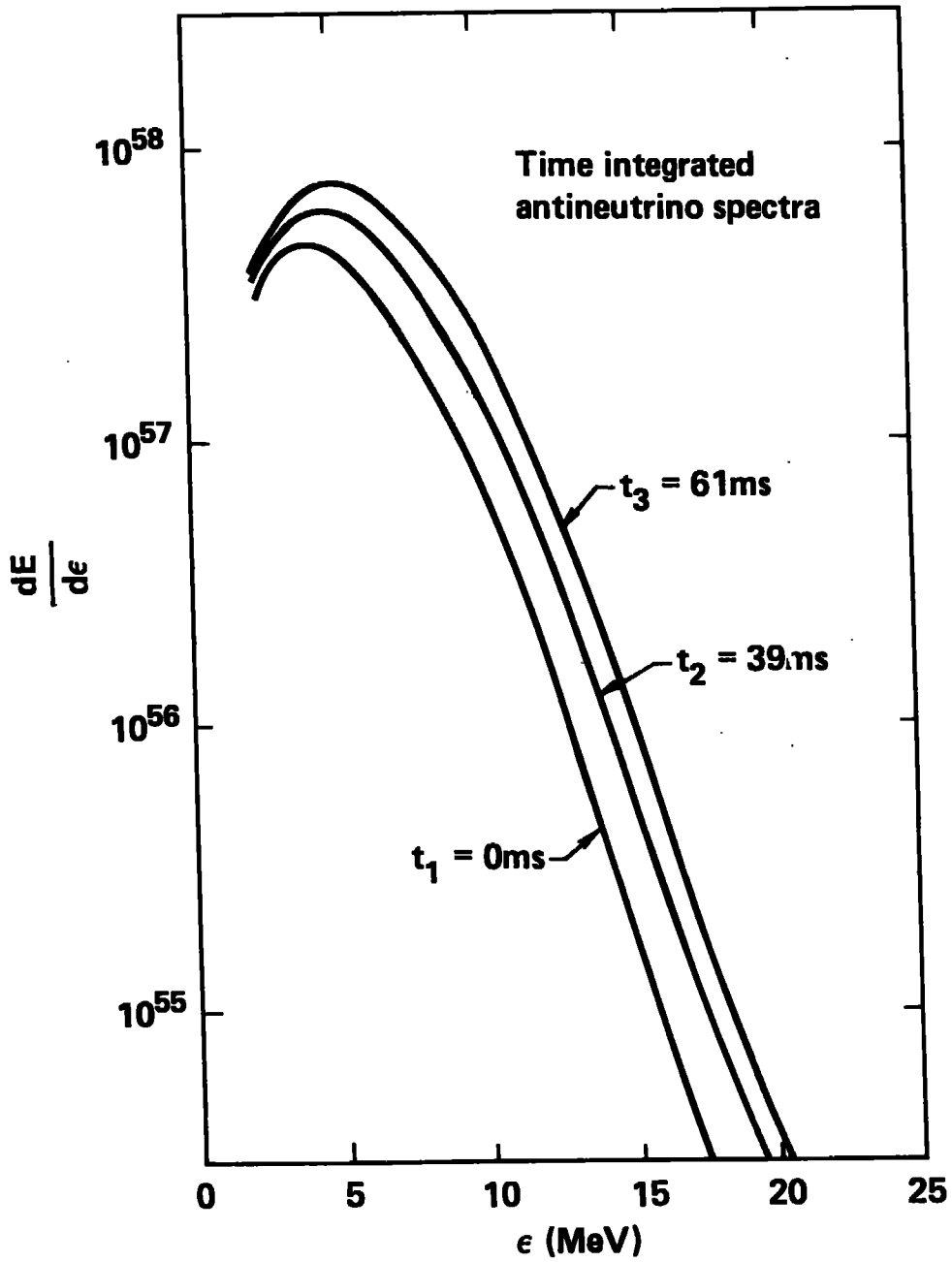
Time integrated
antineutrino spectra
10^{58}
10^{57}
10^{56}
10^{55}
$\frac{dE}{d\epsilon}$
t_3 = 61ms
t_2 = 39ms
t_1 = 0ms
0
5
10
15
20
25
ϵ (MeV)

FIGURE 4

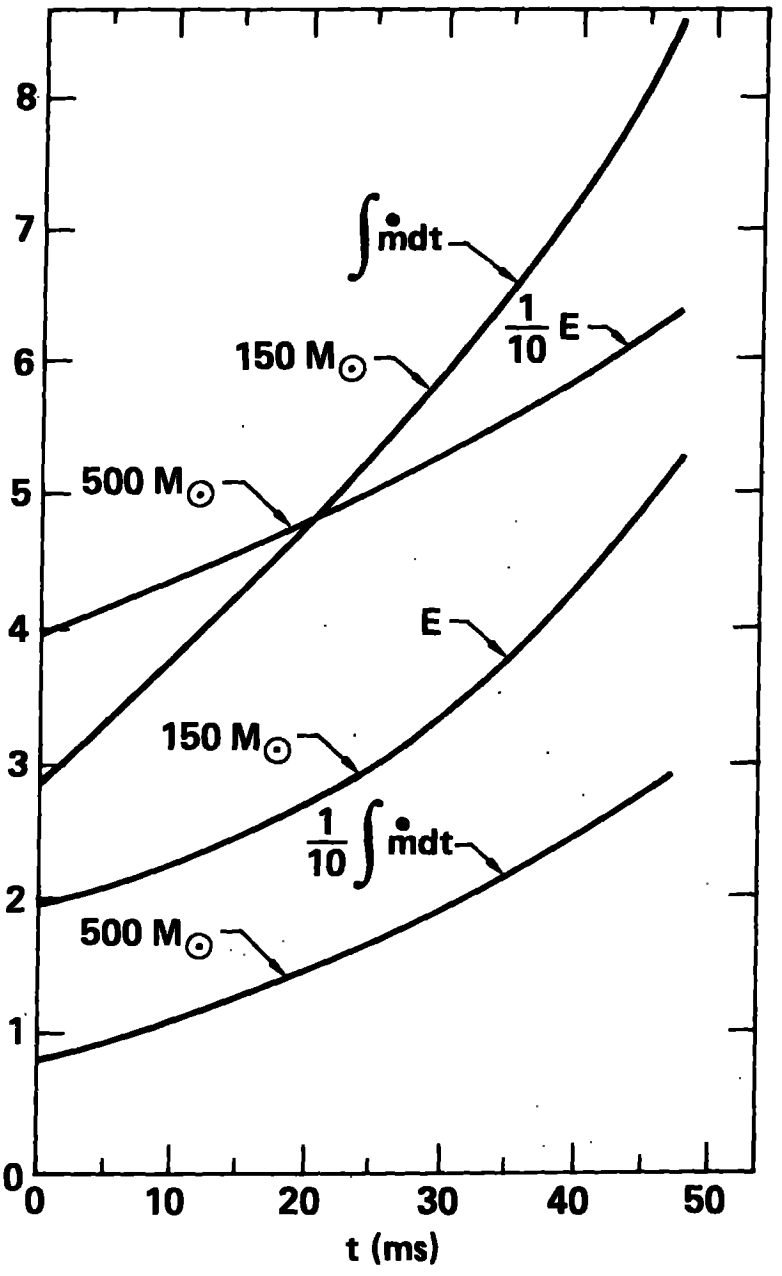
8
7
6
5
4
3
2
1
0
0
10
20
30
40
50
t (ms)
$\int \dot{m} dt$
$\frac{1}{10}$ E
150 $M_\odot$
500 $M_\odot$
E
150 $M_\odot$
$\frac{1}{10} \int \dot{m} dt$
500 $M_\odot$

FIGURE 5

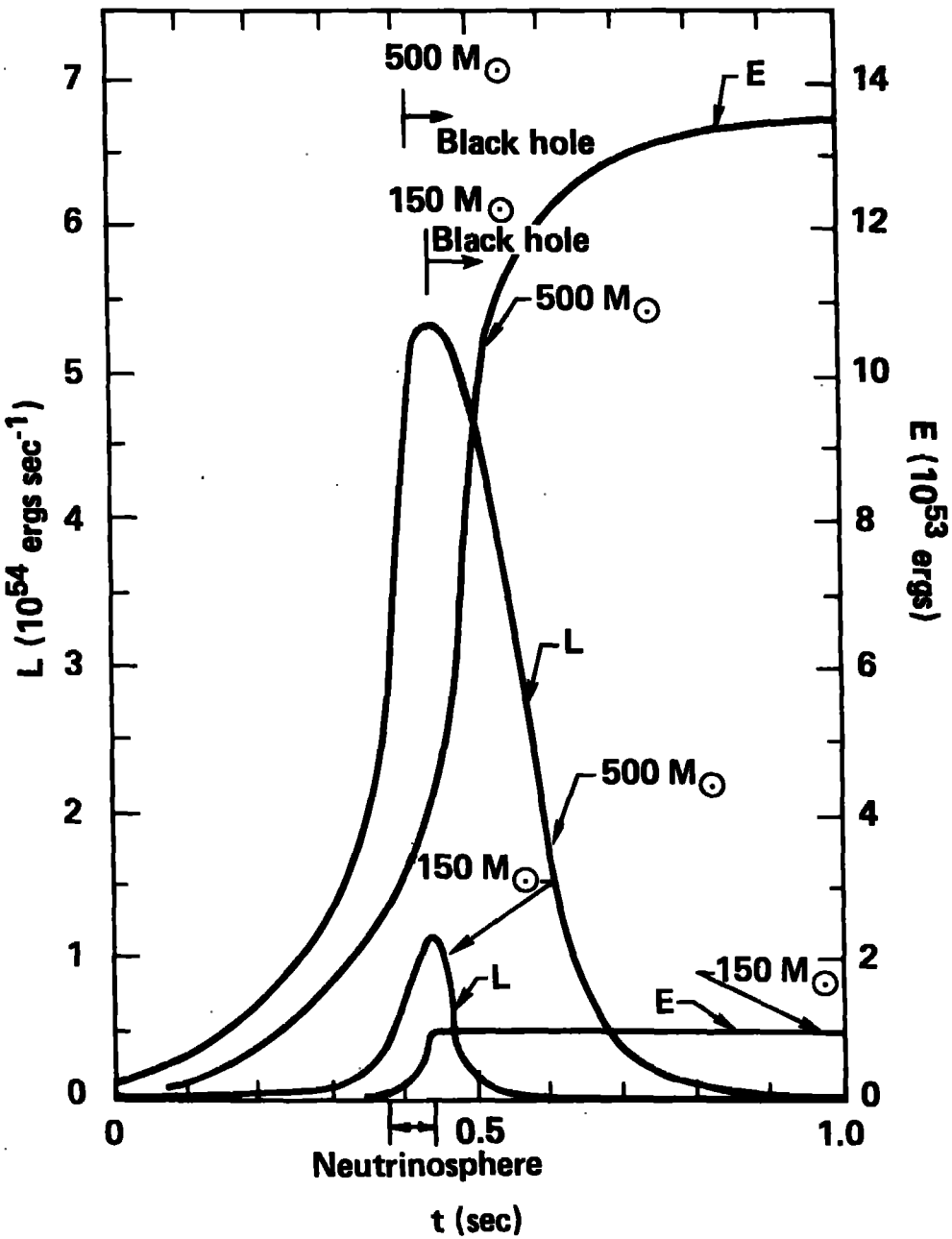
500 M⊙
Black hole
150 M⊙
Black hole
E
500 M⊙
L
500 M⊙
150 M⊙
L
E
150 M⊙
L (10^54 ergs sec^-1)
E (10^53 ergs)
0
1
2
3
4
5
6
7
0
2
4
6
8
10
12
14
0
0.5
1.0
Neutrinosphere
t (sec)

FIGURE 6

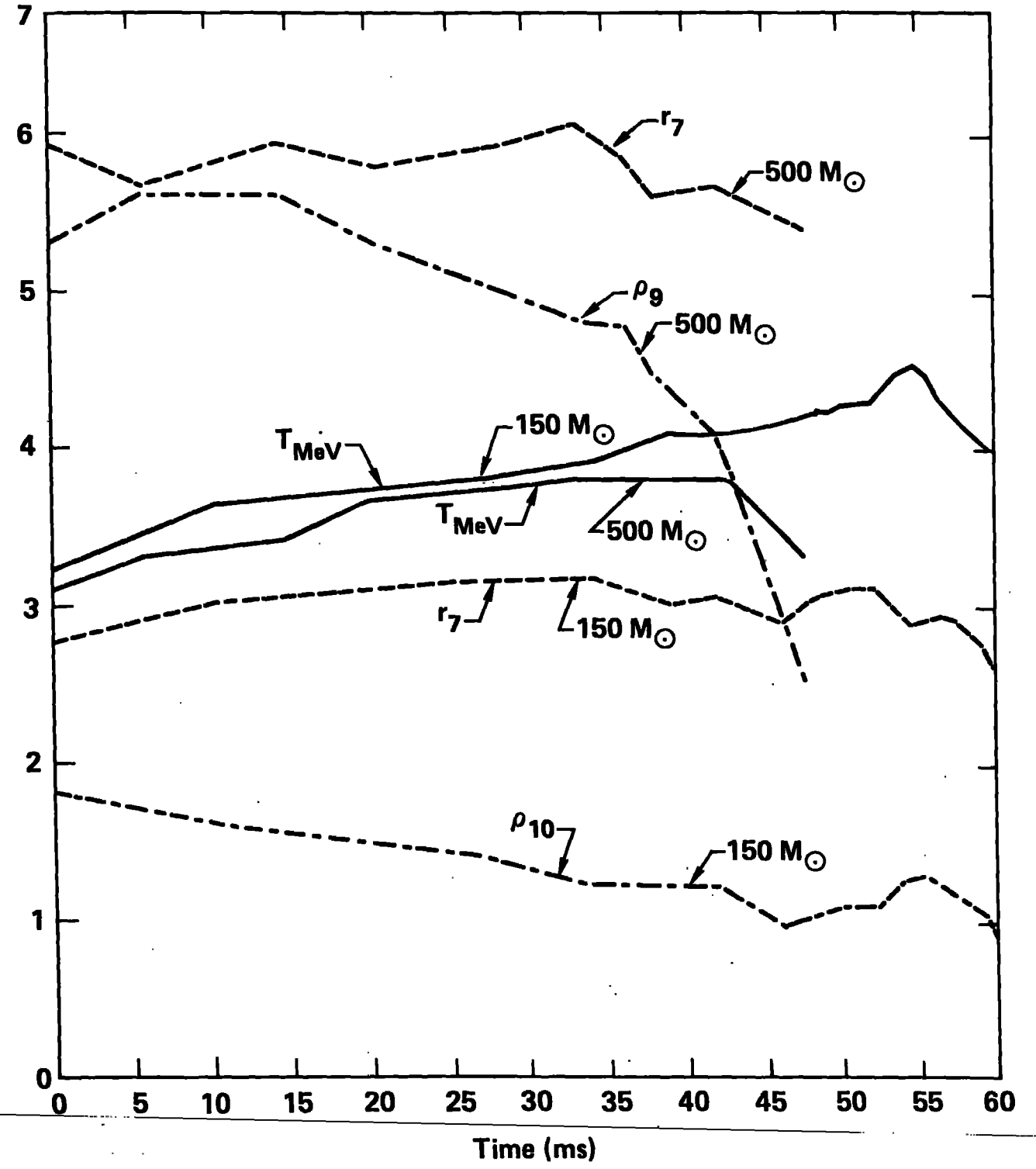
7
6
5
4
3
2
1
0
0
5
10
15
20
25
30
35
40
45
50
55
60
Time (ms)
r_7
500 $M_\odot$
ρ_9
500 $M_\odot$
T_{MeV}
150 $M_\odot$
T_{MeV}
500 $M_\odot$
r_7
150 $M_\odot$
ρ_{10}
150 $M_\odot$

FIGURE 7

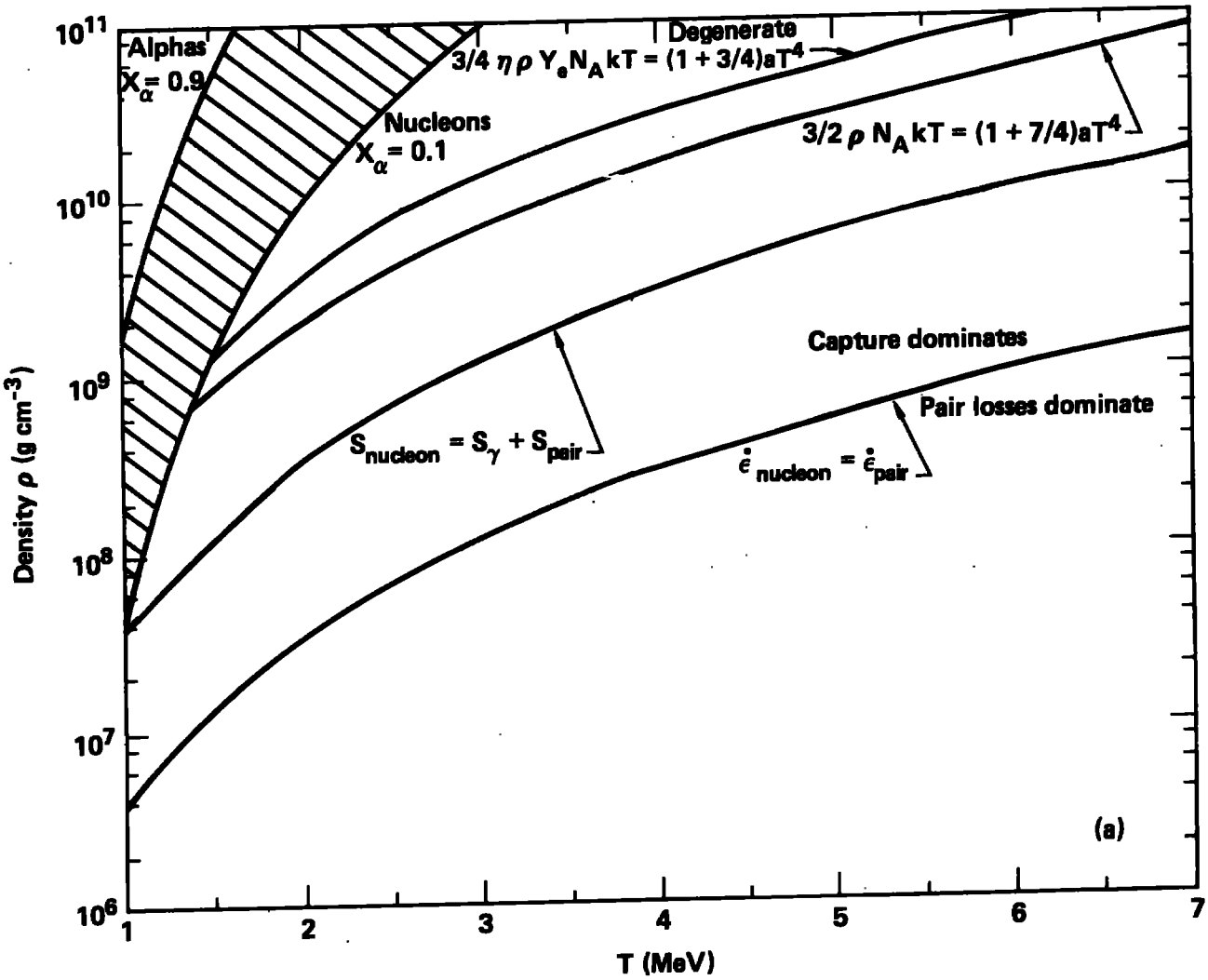
Alphas
$X_\alpha = 0.9$
Nucleons
$X_\alpha = 0.1$
Degenerate
$3/4\ \eta\rho\ Y_e N_A kT = (1 + 3/4)aT^4$
$3/2\ \rho\ N_A kT = (1 + 7/4)aT^4$
Capture dominates
Pair losses dominate
$S_{nucleon} = S_\gamma + S_{pair}$
$\dot{\epsilon}_{nucleon} = \dot{\epsilon}_{pair}$
(a)
Density ρ (g cm^{-3})
10^{11}
10^{10}
10^9
10^8
10^7
10^6
1
2
3
4
5
6
7
T (MeV)

FIGURE 8

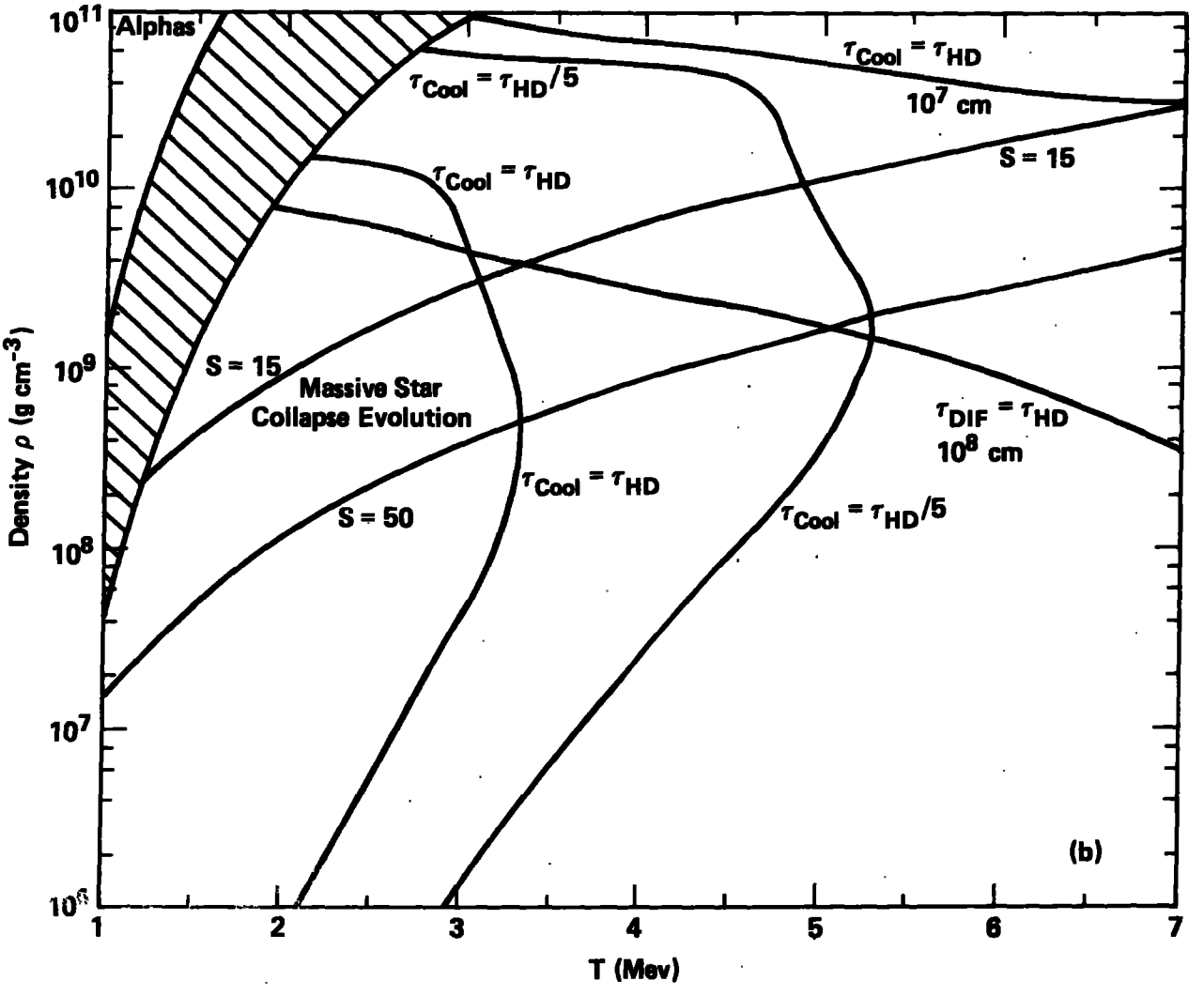
Alphas
$\tau_{Cool} = \tau_{HD}$
$\tau_{Cool} = \tau_{HD}/5$
10^7 cm
$\tau_{Cool} = \tau_{HD}$
S = 15
S = 15
Massive Star
Collapse Evolution
$\tau_{DIF} = \tau_{HD}$
10^8 cm
$\tau_{Cool} = \tau_{HD}$
S = 50
$\tau_{Cool} = \tau_{HD}/5$
(b)
Density ρ (g cm^{-3})
10^{11}
10^{10}
10^9
10^8
10^7
10^6
1
2
3
4
5
6
7
T (Mev)

FIGURE 9

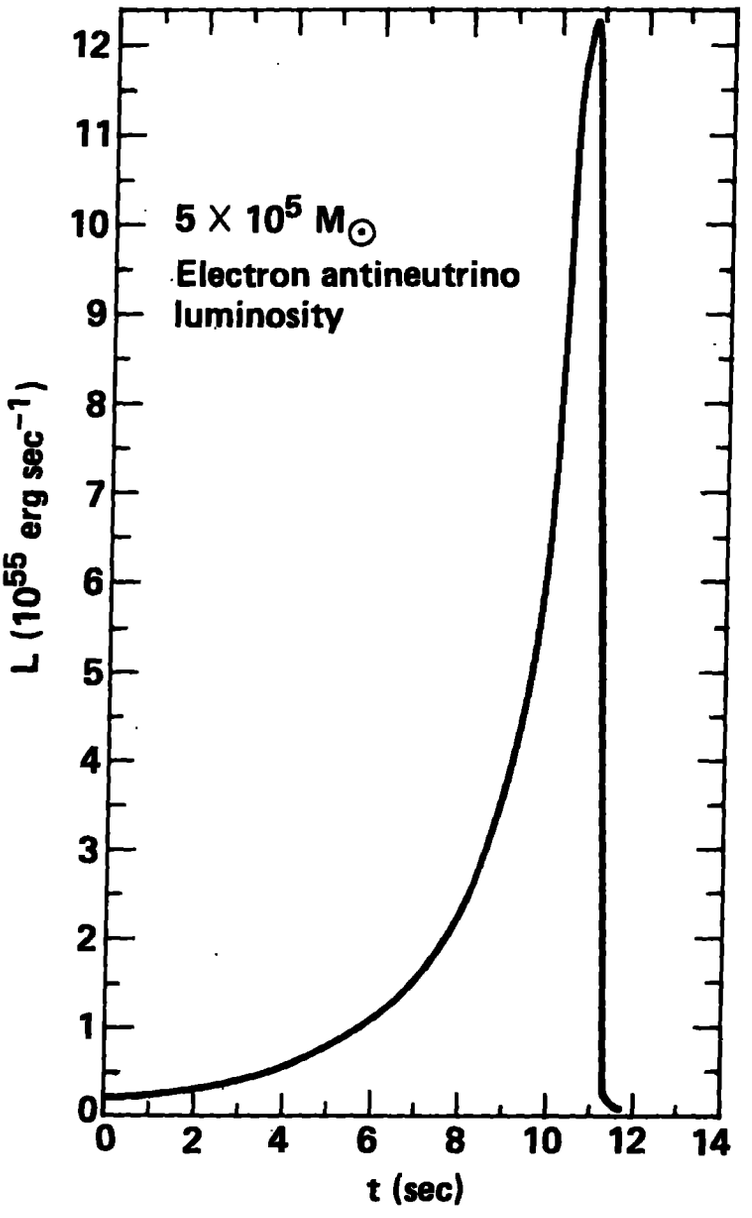
5 X 10^5 M⊙
Electron antineutrino
luminosity
L (10^55 erg sec^-1)
t (sec)
0
1
2
3
4
5
6
7
8
9
10
11
12
0
2
4
6
8
10
12
14

FIGURE 10